CHAPTER IV
RESULTS AND DISCUSSIONS

4.1 Effect of molar ratios of TiO_2 to AC

4.1.1 Formation of crystal with different molar ratios of TiO_2AC composite.

In this work, effects of molar ratios of TiO_2/AC composite on the formation of nanocrystal TiO_2 were investigated. The different molar ratios of TiO_2/AC composite were varied. However, the calcination temperature was kept constant at 500°C. The molar ratios of TiO_2/AC composite included 1:0, 1:10, 1:33, 1:50, 1:70, and 1:100. The crystal structures of TiO_2/AC composite from each ratios obtaining from X-ray diffraction analysis are illustrated in Figure 4.1 and the corresponding surface morphology of TiO_2/AC composite nanocrystals, activated carbon and titanium dioxide are shown in Figure 4.2 (a) – (c)

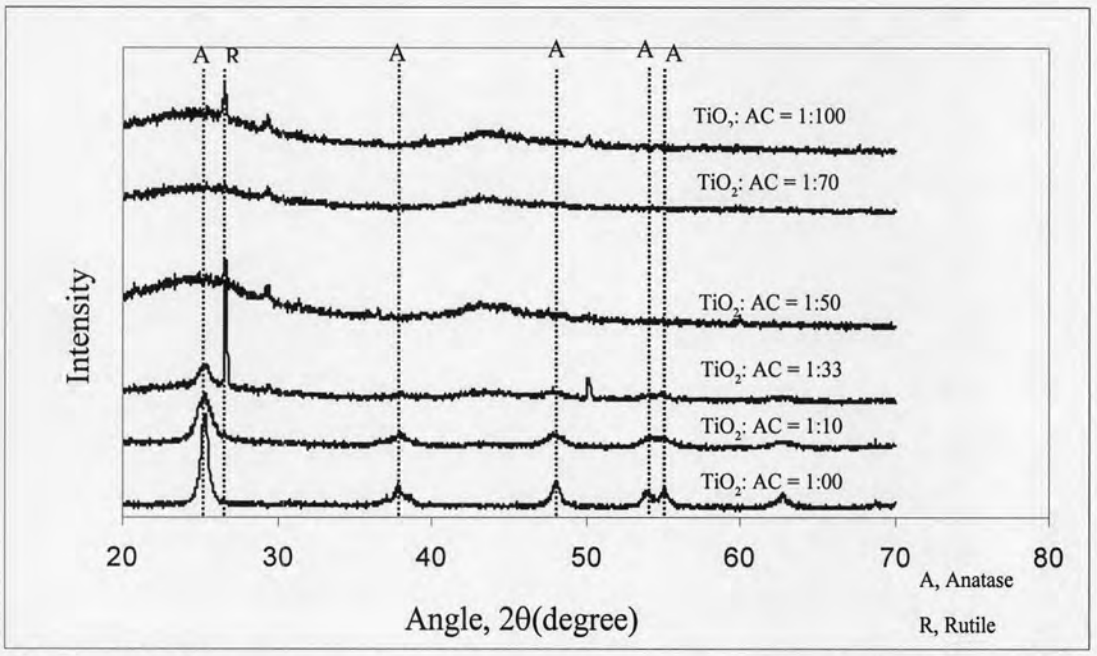

Figure 4.1 XRD spectrum showing crystal structure of TiO_2 obtained from different molar ratios of TiO_2/AC composite.

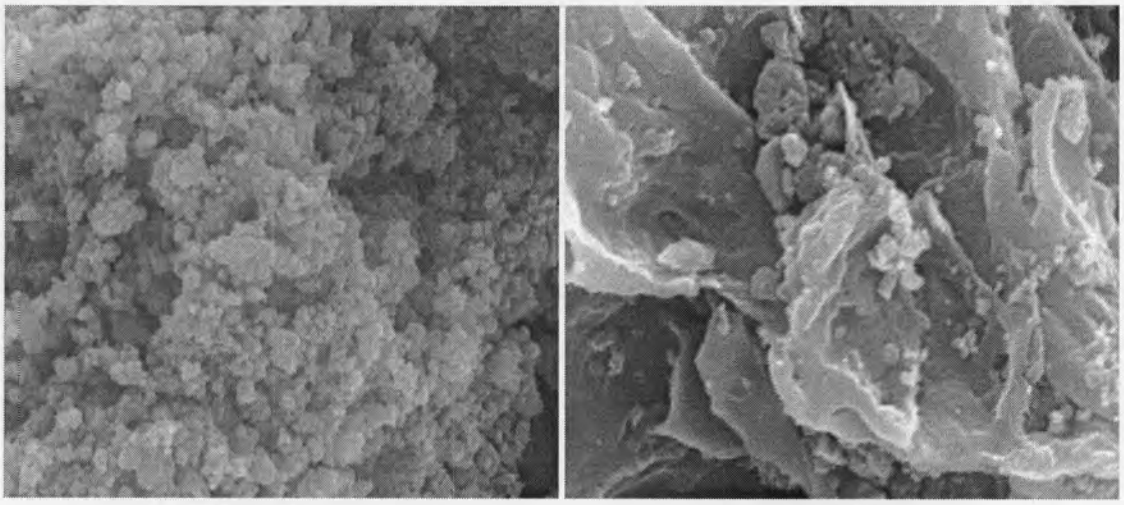

(a) TiO_2 only (b) AC only

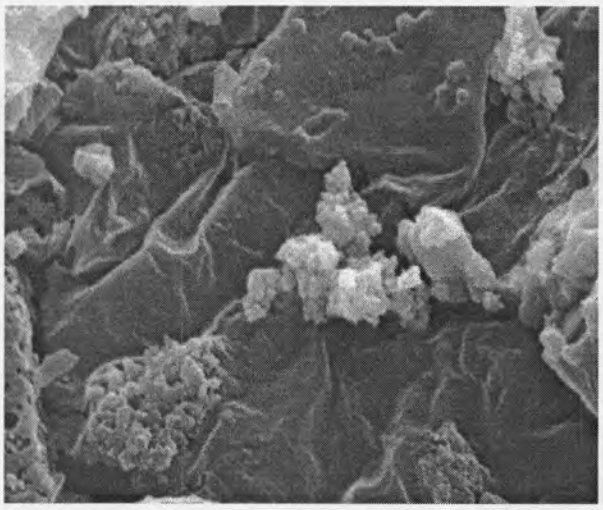

(c) The TiO_2/AC composite

Figure 4.2 SEM images showing surface morphology of TiO_2 nanocrystals obtained from TiO_2, TiO_2/AC, and AC composite.

As shown in the XRD spectrum of TiO_2/AC composite nanoparticles in Figure 4.1, anatase phase was the predominant structure in 1:0 and 1:10 of the molar ratio of TiO_2/AC. A major peak corresponding to (101) reflections of the anatase phase of TiO_2/AC composite was shown at the angle of 25.36°, while the minor peaks were appeared at 48.15° and 54.05°, peak for rutile morphology could be found at the angle of 27.39°.

Moreover, in each molar ratios of TiO_2/AC, phase transformation of anatase to rutile phase with molar ratios of TiO_2:AC 1:33, 1:50, 1:70, and 1:100 as represented

by XRD spectrum of TiO_2/AC composite nanoparticles was detected compared to titanium dioxide. To quantify the phase transformation from anatase to rutile with the different molar ratios of TiO_2/AC composite, the percentage of anatase to rutile was calculated. The phase content of a sample can be calculated from the integvated intensities of the above-mentioned anatase, rutile, and brookite peaks. If a sample contains only anatase and rutile, the weight fraction of rutile (W_R) can be calculated from equation (Gribb and Bamfield, 1997)

$$W_R = \frac{A_R}{0.884A_A + A_R} \qquad \text{(Eq. 4.1)}$$

Where A_A represents the integrated intensity of the anatase (101) peak, and A_R the integrated intensity of rutile (110) peak. If brookite phase is also present in a sample, similar relations can be derived:

$$W_A = \frac{K_A A_A}{K_A A_A + A_R + K_B A_B} \qquad \text{(Eq. 4.2)}$$

$$W_R = \frac{A_R}{K_A A_A + A_R + K_B A_B} \qquad \text{(Eq. 4.3)}$$

$$W_B = \frac{K_B A_B}{K_A A_A + A_R + K_B A_B} \qquad \text{(Eq. 4.4)}$$

Where W_A and W_B represent the weight fraction of anatase and brookite, respectively. A_B is the integrated intensity of the brookite (121) peak, and K_A and K_B are two coefficients to be determined where $K_A = 0.886$ and $K_B = 2.721$ (Zhang and Bamfield, 2000).

Using above equations, the percentage values of anatase to rutile in each condition was calculated and shown in table 4.1.

Table 4.1 Percentages of anatase and rutile phases in samples obtained with different molar ratios of TiO_2/AC

Molar ratios of TiO_2/AC	Anatase (%)	Rutile (%)
1:0	100.00	0.00
1:10	100.00	0.00
1:33	35.36	64.64

It was found that the percentage of anatase of TiO_2 was 100%. With AC in the molar ratio of TiO_2/AC in 1:10 and 1:33, the percentage ratios of anatase: rutile were changed to be 100.00:0.00 and 35.36: 64.64, respectively. Moreover, in the molar ratio of TiO_2/AC in 1:50, 1:70, and 1:100, formation of anatase phase was not predominant with a small portion of rutile presented. Owing to application of TiO_2/AC in this work was used as photocatalyst, the major crystal phase as anatase was required. The TiO_2/AC with molar ratio as 1:10 was selected for further experiments.

4.1.2 Comparison of the photocatalytic process TiO_2/N_2, TiO_2/O_2, and $TiO_2/AC/N_2$

In this part, TiO_2/N_2 represents TiO_2 calcined at 500°C under N_2 gas, TiO_2/O_2 was TiO_2 calcined at 500°C under O_2 atmosphere, $TiO_2/AC/N_2$ was TiO_2/AC calcined at 500°C under N_2 gas and AC/N_2 was AC calcined at 500°C under N_2 gas. All materials were taken for photocatalytic activity test. The comparison of adsorption and photocatalytic were performances of these materials were shown as follow:

4.1.2.1 Determination of 2-CP adsorption on TiO_2/N_2, TiO_2/O_2, and $TiO_2/AC/N_2$ surface

Comparison of 2-CP adsorption using TiO_2/N_2, $TiO_2/AC/N_2$, AC/N_2 and TiO_2/O_2 is shown in Figure 4.3. From this graph, activated carbon (AC/N_2) provide the highest adsorption of 2-CP. While the pure titanium dioxide synthesized under oxygen atmosphere (TiO_2/O_2) provide the lowest 2-CP adsorption. The adsorption ability of all materials are sequence as $AC/N_2 > TiO_2/AC/N_2 > TiO_2/N_2 > TiO_2/O_2$. It is clearly that activated carbon in $TiO_2/AC/N_2$ enhanced the adsorption ability in the composite material.

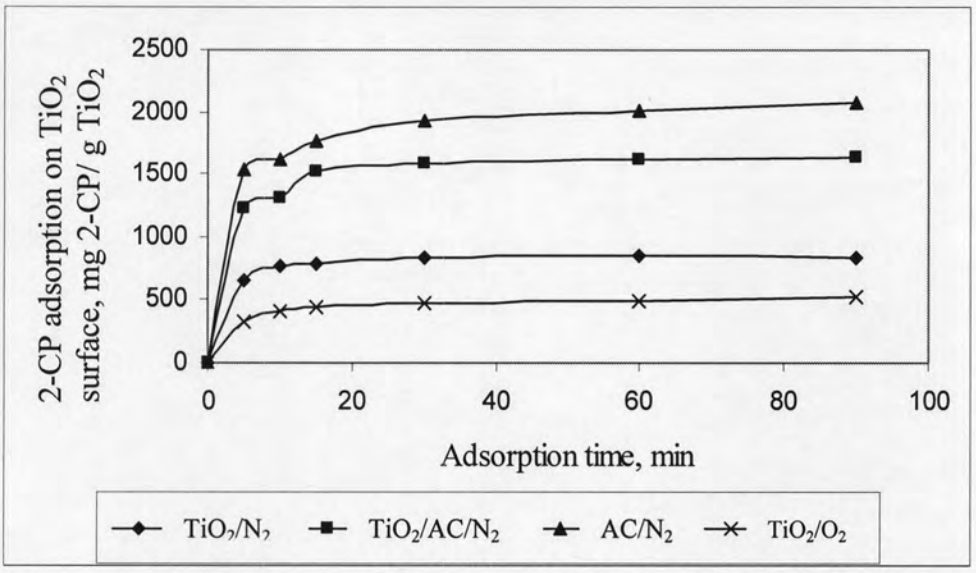

Figure 4.3 Comparison of the 2-CP adsorption on TiO_2/O_2, TiO_2/N_2, $TiO_2/AC/N_2$, and AC/N_2 surface

4.1.2.2 Determination of Adsorption Isotherm of TiO_2/O_2

To obtain the adsorption isotherm of TiO_2/O_2 composite, the plot of adsorbed 2-CP on titania surface versus the concentration of 2-CP in the solution after reaching the equilibrium was performed as shown in Figure 4.4. The value of adsorbed 2-CP on titania surface was increased with increasing of 2-CP initial concentrations and the plateau of the adsorption pattern was obtained.

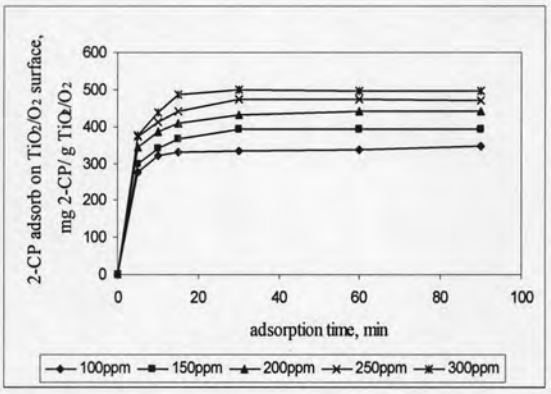

(a) Adsorption of 2-CP on the surface of TiO_2/O_2

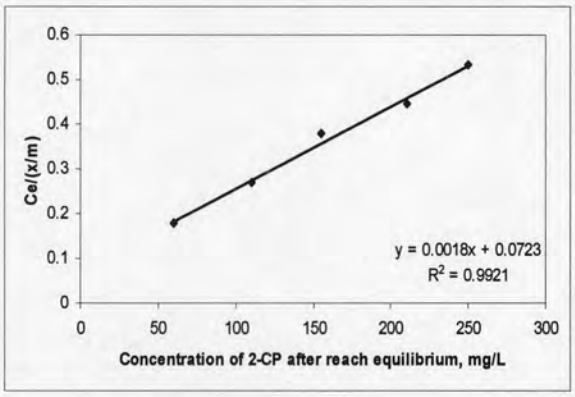

(b) Langmuir adsorption isotherm

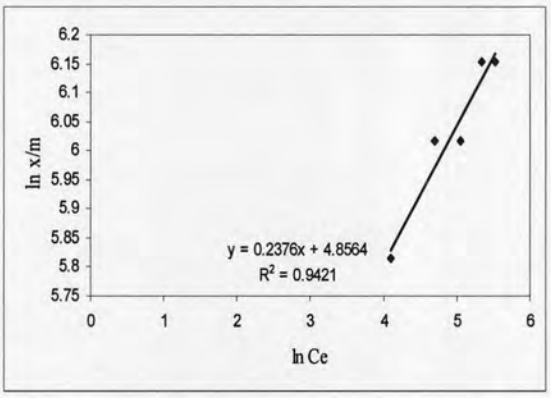

(c) Freundlich adsorption isotherm

Figure 4.4 Adsorption of 2-CP on the surface of TiO_2/O_2 composite, Langmuir adsorption isotherm and Freundlich adsorption isotherm at different initial concentration of 2-CP as a function of time in (a), (b), and (c), respectively.

The values of 2-CP adsorption at the equilibrium condition were used further in determining the adsorption isotherm in both Langmuir and Freundlich equations.

The Langmuir equation was applied for the adsorption equilibrium of 2-CP onto TiO_2/AC composite surface. The Langmuir adsorption isotherm is based on these assumptions:

(i) maximum adsorption corresponds to a saturated monolayer of adsorbate molecules on the adsorbent surface;

(ii) the energy of adsorption is constant;

(iii) There is no transmigration of adsorbate in the surface plane.

The Langmuir equation is shown below:

$$\frac{C_e}{(x/m)} = \frac{1}{(Q_0 b)} + \frac{C_e}{Q_0} \qquad \text{(Eq. 4.5)}$$

Where C_e is the equilibrium concentration of 2-CP, mg/L, (x/m) is the amount of adsorbed 2-CP at equilibrium per unit mass of TiO_2, mg/g, and Q_0 and b are Langmuir constants related to adsorptive capacity and energy of adsorption, respectively.

The linear plot of C_e/(x/m) vs. C_e in Figure 4.4 shows that the adsorption of 2-CP onto the TiO_2/AC composite surface obeys the Langmuir adsorption isotherm.

The freundlich equation was also applied to describe the adsorption of 2-CP onto the TiO_2/AC composite surface. The Freundlich equation is basically empirical, and generally agrees with the experimental data over a moderate range of adsorbate concentrations. The Freundlich isotherm is represented by the equation (Mckay et al., 1982)

$$\ln (x/m) = (1/n)\ln Ce + \ln K_f \qquad \text{(Eq. 4.6)}$$

Where C_e is the equilibrium concentration of 2-CP, mg/L, (x/m) is the amount of adsorbed 2-CP at equilibrium per unit mass of TiO_2/AC composite, mg/g, and K_f and n are the Freundlich constants.

The linear plot of ln(x/m) vs. $\ln C_e$ in Figure 4.4 shows that adsorption of 2-CP onto the TiO_2/AC composite surface obeys the Freundlich adsorption isotherm.

Table 4.2 Langmuir and Freundlich equation of TiO_2/O_2 composite at 500°C calcination temperature and 300 mg/L as initial concentration

Type of TiO_2 and AC	Langmuir equation	R^2	Freundlich equation	R^2
TiO_2/O_2	Y=0.0018x+0.0723	0.9921	Y=0.2376x+4.8564	0.9421

From data in the table 4.2 shows that, the adsorption behavior of TiO_2/O_2 is followed the Langmuir equation. The adsorption behavior of 2-CP onto TiO_2/O_2 tends to be a monolayer adsorption as described by the Langmuir isotherm rather than the Freundlich isotherm.

4.1.2.3 Determination of Adsorption Isotherm of TiO_2/N_2

To obtain the adsorption isotherm of TiO_2/N_2 composite, the plot of adsorbed 2-CP on titania surface versus the concentration of 2-CP in the solution after reaching the equilibrium was performed as shown in Figure 4.5. The value of adsorbed 2-CP on titania surface was increased with increasing of 2-CP initial concentrations and the plateau of the adsorption pattern was obtained.

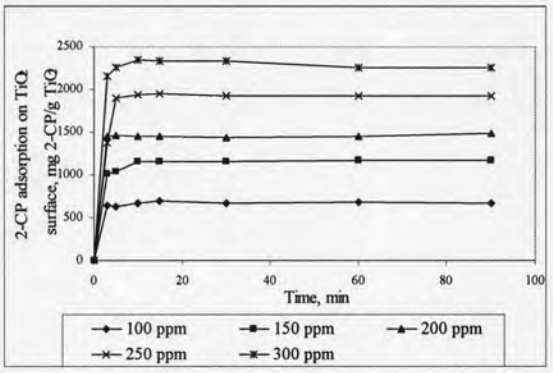

(a) Adsorption of 2-CP on the surface of TiO_2/N_2

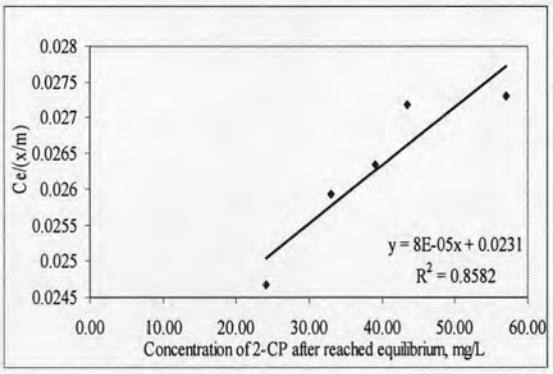

(b) Langmuir adsorption isotherm

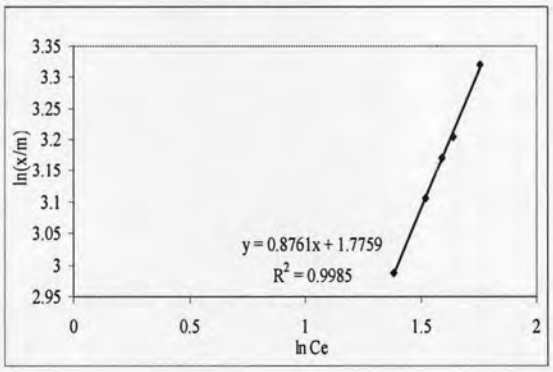

(c) Freundlich adsorption isotherm

Figure 4.5 Adsorption of 2-CP on the surface of TiO_2/N_2 composite, Langmuir adsorption isotherm and Freundlich adsorption isotherm at different initial concentration of 2-CP as a function of time in (a), (b), and (c), respectively.

Table 4.3 Langmuir and Freundlich equation of TiO_2/N_2 composite at 500°C calcination temperature and 300 mg/L as initial concentration

Type of TiO_2 and AC	Langmuir equation	R^2	Freundlich equation	R^2
TiO_2/N_2	Y=8E-05x+0.0231	0.8582	Y=0.8761x+1.7759	0.9985

From data in the table 4.3 shows that, the adsorption behavior of TiO_2/N_2 followed the Freundlich equation. The adsorption behavior of 2-CP onto TiO_2/N_2 tends to be a multilayer adsorption as described by the Freundlich isotherm rather than the Langmuir isotherm. It might be explained that the N_2 might influence the adsorption behavior of TiO_2 from the monolayer adsorption to multilayer adsorption. Thus, the TiO_2/N_2 has tendency to provide higher efficiency in adsorption than TiO_2/O_2 as shown in previous part.

4.1.2.4 Determination of Adsorption Isotherm of $TiO_2/AC/N_2$

To obtain the adsorption isotherm of $TiO_2/AC/N_2$ composite, the plot of adsorbed 2-CP on titania surface versus the concentration of 2-CP in the solution after reaching the equilibrium was performed as shown in Figure 4.6. The value of adsorbed 2-CP on titania surface was increased with increasing of 2-CP initial concentrations and the plateau of the adsorption pattern was obtained.

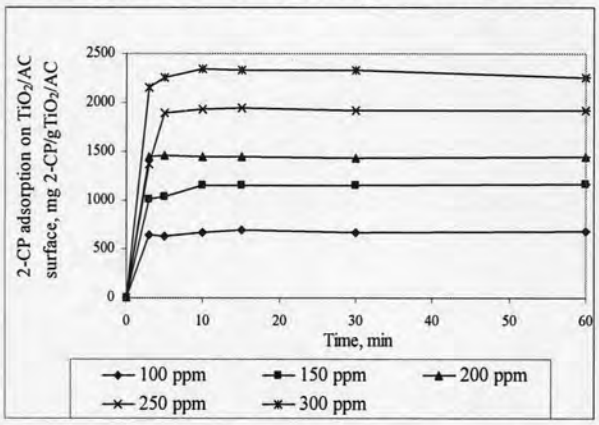

(a) Adsorption of 2-CP on the surface of $TiO_2/AC/N_2$

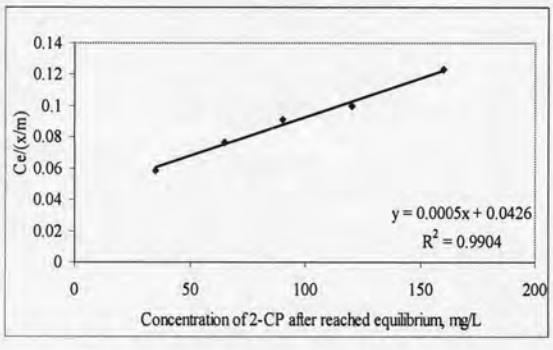

(b) Langmuir adsorption isotherm

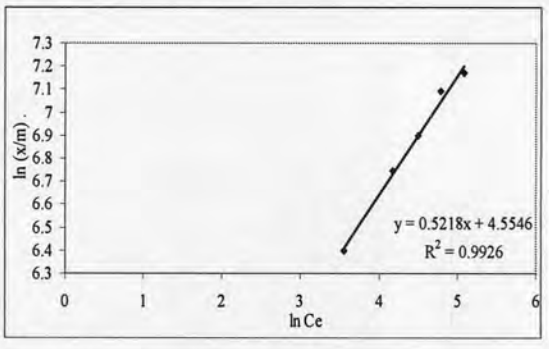

(c) Freundlich adsorption isotherm

Figure 4.6 Adsorption of 2-CP on the surface of $TiO_2/AC/N_2$ composite, Langmuir adsorption isotherm and Freundlich adsorption isotherm at different initial concentration of 2-CP as a function of time in (a), (b), and (c), respectively.

Table 4.4 Langmuir and Freundlich equation of $TiO_2/AC/N_2$ composite at 500°C calcination temperature and 300 mg/L as initial concentration

Type of TiO_2 and AC	Langmuir equation	R^2	Freundlich equation	R^2
$TiO_2/AC/N_2$	Y=0.0004x+0.0442	0.9904	Y=0.5865x+4.3196	0.9926

From data in the table 4.4, the adsorption behavior of $TiO_2/AC/N_2$ followed the Freundlich equation. The adsorption behavior of 2-CP onto $TiO_2/AC/N_2$ tends to be a multilayer adsorption as described by the Freundlich isotherm rather than the Langmuir isotherm. From the fact adsorption behavior of AC is followed the Freundlich pattern and, in the previous part, TiO_2/N_2 has the adsorption isotherm followed the Freundlich equation. When TiO_2/N_2 was deposited on AC, the $TiO_2/AC/N_2$ composite was high tendency to be explained by the Freundlich adsorption isotherm.

4.1.2.4 Determination of Adsorption Isotherm of AC/N_2

To obtain the adsorption isotherm of TiO_2/AC composite, the plot of adsorbed 2-CP on titania surface versus the concentration of 2-CP in the solution after reaching the equilibrium was performed as shown in Figure 4.7. The value of adsorbed 2-CP on titania surface was increased with increasing of 2-CP initial concentrations and the plateau of the adsorption pattern was obtained.

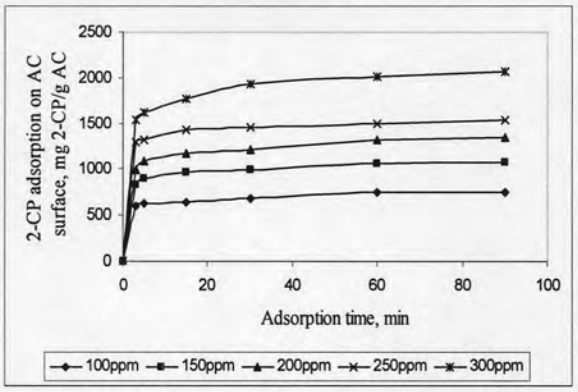

(a) Adsorption of 2-CP on the surface of AC/N_2

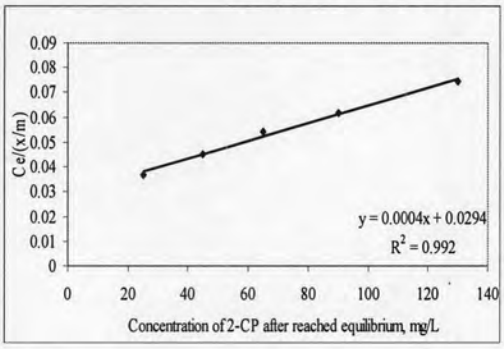

(b) Langmuir adsorption isotherm

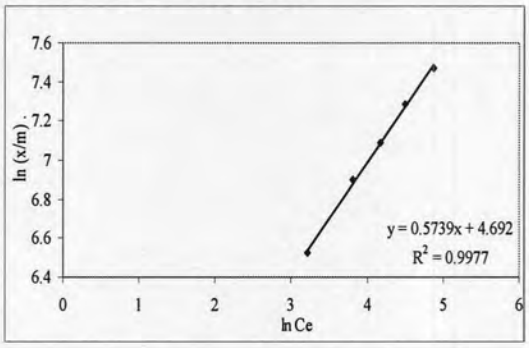

(c) Freundlich adsorption isotherm

Figure 4.7 Adsorption of 2-CP on the surface of AC/N_2 composite, Langmuir adsorption isotherm and Freundlich adsorption isotherm at different initial concentration of 2-CP as a function of time in (a), (b), and (c), respectively.

Table 4.5 Langmuir and Freundlich equation of AC/N_2 composite at 500°C calcination temperature and 300 mg/L as initial concentration

Type of TiO_2 and AC	Langmuir equation	R^2	Freundlich equation	R^2
AC/N_2	Y=0.0004x+0.0294	0.9920	Y=0.5739x+4.692	0.9977

From data in the table 4.5 shows that, the adsorption behavior of AC/N_2 followed the Freundlich equation. The adsorption behavior of 2-CP onto AC/N_2 tends to be a multilayer adsorption as described by the Freundlich isotherm rather than the Langmuir isotherm.

4.1.2.5 Comparison of Adsorption Isotherm of TiO_2/O_2, TiO_2/N_2, $TiO_2/AC/N_2$ and AC/N_2

The comparison of adsorption isotherm of TiO_2/O_2, TiO_2/N_2, $TiO_2/AC/N_2$ and AC/N_2 is shown in table 4.6

Table 4.6 The comparison of Adsorption Isotherm of TiO_2/O_2, TiO_2/N_2, $TiO_2/AC/N_2$ and AC/N_2

Type of TiO_2/AC	Adsorption Isotherm	Equation	Constant
TiO_2/O_2	Langmuir	Y=0.0018x+0.0723	Q_0= 555.556, and b= 0.0249
TiO_2/N_2	Freundlich	Y=0.8761x+1.7759	k_f = 0.5743, and n= 1.1414
$TiO_2/AC/N_2$	Freundlich	Y=0.5865x+4.3196	k_f= 1.4632, and n= 1.7050
AC/N_2	Freundlich	Y=0.5739x+4.692	k_f = 1.5458, and n= 1.7425

This experiment shows that the TiO_2/N_2, $TiO_2/AC/N_2$, and AC/N_2 were followed Freundlich adsorption isotherm. The TiO_2/N_2, $TiO_2/AC/N_2$, and AC/N_2 have more efficiency in adsorption activity than that in TiO_2/O_2. The adsorption efficiency in 2-CP removal is ordered as AC/N_2 > $TiO_2/AC/N_2$ > TiO_2/N_2 > TiO_2/O_2. It was found that, the composite materials that have combined TiO_2 with AC have more efficiency owing to the enhancement of adsorption behavior by activated carbon.

4.1.2.6 Irradiation process of TiO_2/O_2, TiO_2/N_2, $TiO_2/AC/N_2$ and TiO_2/P-25

To investigate the effect of nanocrystal TiO_2, TiO_2/O_2, TiO_2/N_2, $TiO_2/AC/N_2$ and TiO_2/P-25 were studied on removal of hazardous wastes from the wastewater. The synthesized TiO_2/O_2, TiO_2/N_2, $TiO_2/AC/N_2$ and TiO_2/P-25 composite were used in the photocatalysis process of 2–CP removal from the synthetic wastewater.

In general, the photocatalytic process involves different processes including adsorption – desorption, electron–hole pair production and recombination, and chemical conversion (Demeestere et al., 2004). Since recombination of photogenerated electron–hole pairs occurs within a fraction of a nanosecond, charge separation is only kinetically competitive if trapping species are already absolved

prior to electron-hole pair generation (Fox and Dulay, 1993; Alberici and Jardim, 1997; Wittmam et al., 2005).

To explain the behavior of photocatalytic oxidation of 2-CP by the synthesized TiO_2/O_2, TiO_2/N_2, $TiO_2/AC/N_2$ composite in term of kinetic study, two patterns of kinetic orders, which are zero-order and pseudo-first order equations, are considered. As can be seen in the 2-CP declining pattern, the kinetic order to explain the existing reaction can be either zero-order or pseudo-first order. Thus, the value of k_{obs} can be calculated by both equations

The zero-order equation can be derived as follows:

$$\frac{dC}{dt} = -k[C]^0 = -k \qquad \text{(Eq. 4.7)}$$

$$dC = -k(dt) \qquad \text{(Eq. 4.8)}$$

$$\int_{C_0}^{C} dC = -k \int_{0}^{t} dt \qquad \text{(Eq. 4.9)}$$

$$C - C_0 = -k_{obs}t \qquad \text{(Eq. 4.10)}$$

Where k_{obs} is the apparent reaction rate constant, t is the reaction time, C_0 is the initial concentration of 2-CP in aqueous solution, and C is the residual concentration of 2-CP at time t. Value of k_{obs} was determined from the slope of graph which was plotted between $C-C_0$ and reaction time, t. The value R^2 for linear regression was calculated to exhibit the tendency of the reaction pattern to be a zero-order pattern. Values of k_{obs} from zero-order equation were determined.

The pseudo-first order equation can be obtained by the following relationship of C and t:

$$\frac{d[C]}{dt} = -k_{obs}[C]^n = -k_{obs}[C]^1 \qquad \text{(Eq. 4.11)}$$

$$\frac{1}{[C]}d[C] = -k_{obs}dt \qquad \text{(Eq. 4.12)}$$

$$\int_{C_0}^{C} \frac{1}{[C]}d[C] = -\int_{0}^{t} k_{obs}dt \qquad \text{(Eq. 4.13)}$$

$$\ln\left(\frac{C}{C_0}\right) = -k_{obs}t \qquad \text{(Eq. 4.14)}$$

Where k_{obs} is the apparent reaction rate constant, t is the reaction time, C_0 is the initial concentration of 2-CP in the aqueous solution, and C is the residual concentration of 2-CP at time t. Value of k_{obs} was determinined from the slope of graph which was plotted between $C-C_0$ and reaction time, t. The value R^2 for linear regression was calculated to exhibit the tendency of the reaction pattern to be a zero-order pattern. Values of k_{obs} from zero-order equation were determined and show in figure 4.8 and 4.9.

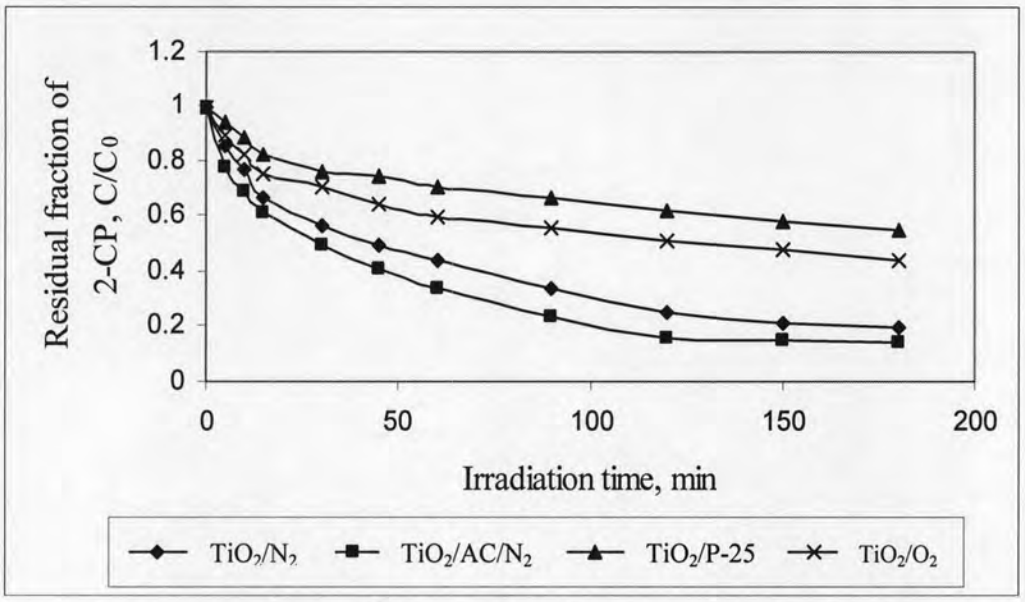

Figure4.8 Photocatalytic oxidation of 2-CP by using TiO_2/O_2, TiO_2/N_2, $TiO_2/AC/N_2$and TiO_2/P-25 at 500°C as calcination temperature and 300 mg/L as initial concentration

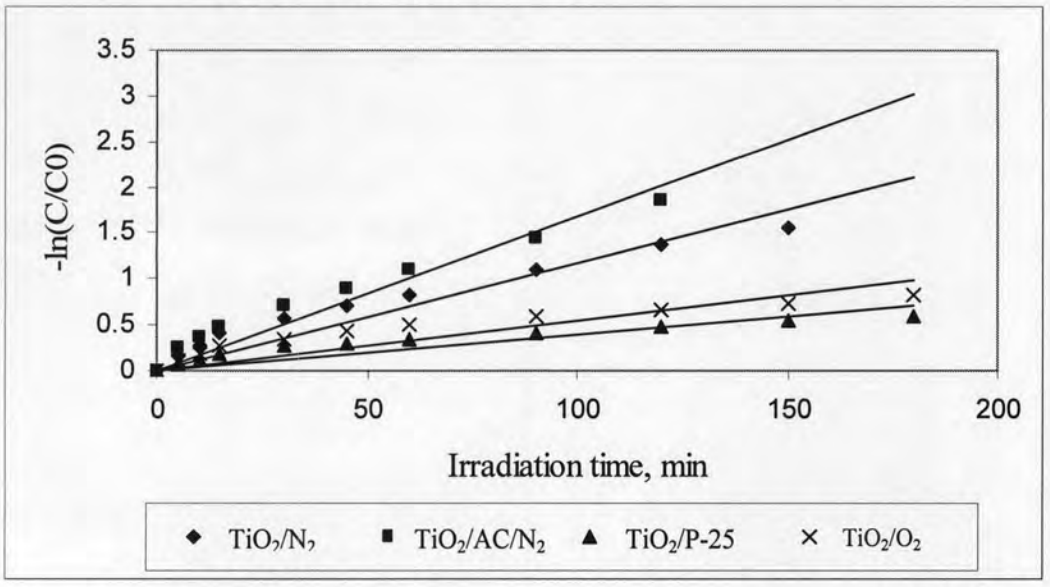

Figure 4.9 Value of k_{obs} from the photocatalytic process of removal 2-CP by using TiO_2/O_2, TiO_2/N_2, $TiO_2/AC/N_2$and TiO_2/P-25 at 500°C as calcination temperature and 300 mg/L as initial concentration

To study the kinetics of the photocatalysis process. The observed kinetic constant, k_{obs}, from each experimental condition was also calculated. Considering the pattern of kinetic equation, the reaction behavior of nanocrystal TiO_2/AC composite in 2–CP removal was followed the first–order pattern and show in table 4.7.

Table 4.7 Value of k_{obs} and 2–CP removal efficiencies of TiO_2/O_2, TiO_2/N_2, TiO_2/AC/$N_2$and TiO_2/P-25 prepare at 500°C as calcination temperature and 300 mg/L as initial concentration

Type of TiO_2 and AC	k_{obs}	R^2	% Removal
TiO_2/N_2	0.0116	0.9998	80.11
TiO_2/AC/N_2	0.0168	0.9906	86.27
TiO_2/P-25	0.0099	0.9738	45.42
TiO_2/O_2	0.0099	0.9815	55.85

This comparison shows that in the 2-CP removal efficiency using TiO_2 catalyst can be sequence as TiO_2/AC/$N_2 \cong TiO_2/N_2 > TiO_2/O_2 \cong TiO_2$/P-25. Results from this part showed that TiO_2/N_2 and TiO_2/AC/N_2 provided higher efficiency than TiO_2/O_2 and TiO_2/P-25. Apparantly, the TiO_2/AC/N_2 has higher efficiency than TiO_2/N_2. From this work, it is clearly shown that AC enhanced high adsorption on the surface of TiO_2 leading to high efficiency in photocatalytic process.

4.1.2.7 Photocatalysis process of TiO_2/O_2, TiO_2/N_2, $TiO_2/AC/N_2$ and TiO_2/P-25

The whole photocatalytic process concluding with the adsorption part and Irradiation part were experimented using TiO_2/O_2, TiO_2/N_2, $TiO_2/AC/N_2$, and TiO_2/P-25. The results are shown in figure 4.10.

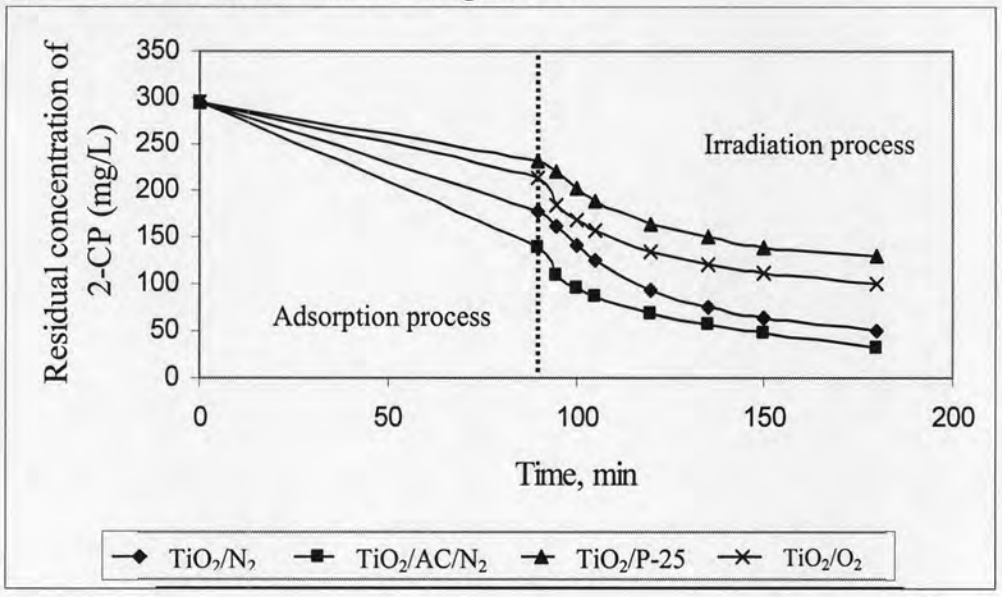

Figure 4.10 Comparison of the Adsorption and Irradiation of TiO_2/O_2, TiO_2/N_2, $TiO_2/AC/N_2$and TiO_2/P-25

4.1.2.8 Comparison of the efficiency of all composite in 2-CP removal

The comparison of the efficiency in 2-CP removal for all materials is shown in table 4.8;

Table 4.8 Comparison of the efficiency in 2-CP removal

Type of TiO_2 composite	Process in 270 min.	% of 2-CP removal
AC	Adsorption process	70.62
TiO_2/O_2	Irradiation process	71.53
TiO_2/N_2	Irradiation process	78.99
$TiO_2/AC/N_2$	Irradiation process	93.51
TiO_2/P-25	Irradiation process	67.31

From graph, $TiO_2/AC/N_2$ provided highest efficiency in photocatalysis process. The 2-CP removal efficiency using all materials are ordered as $TiO_2/AC/N_2$ > TiO_2/N_2 > TiO_2/O_2 > TiO_2/P-25. With the enhancing of activated carbon, the 2-CP can adsorb on the TiO_2 surface leading to high efficiency in photocatalysis process. It is obvious that the nanocrystal TiO_2/AC composite prepared at 500°C calcination

temperature provided the highest efficiency in 2-CP removal compared to the other conditions. It is worth to note that the TiO_2/AC composite in the molar ratio of 1:10 with 500°C calcination temperature provided the highest amount of 2–CP adsorption on titania surface, while the TiO_2/AC composite with 500°C calcination temperature provided the highest amount of 2–CP reduction upon irradiation process

4.1.2.9 Determination of kinetic values following Langmuir- Hinshelwood model for TiO_2/O_2, TiO_2/N_2, $TiO_2/AC/N_2$ and TiO_2/P-25

Additional kinetic values were obtained using Langmuir-Hinshelwood model. The best condition from the previous section was used in this part. The photocatalytic oxidation of 2-CP by TiO_2/O_2, TiO_2/N_2, $TiO_2/AC/N_2$, and TiO_2/P-25 composite with variation of initial concentrations of 2-CP in the range of 100-300 mg/L were conducted.

The reaction was dependent only on the reaction time and it was independent from the concentration of 2-CP in the aqueous solution. The surface of titania is not the limitation of the reaction. As 2-CP concentration increased with the fixed dosage of TiO_2/AC composite in the system, the reaction became dependent on both concentration of 2-CP and the reaction time. Results from this experiment set provide the important information that at low level of contaminant concentration, the reaction is best described by pseudo first-order pattern.

The value of k_{obs} obtained from the pseudo first-order pattern can be used further to find the intrinsic kinetic values of photocatalysis can be determined from the Langmuir-Hinshelwood model. In this model, the reaction rate for second-order surface decomposition of 2-CP can be represented as:

$$\text{rate} = -\frac{d[2-CP]}{dt} = k_C \frac{K_{2-CP}[2-CP]}{1+K_{2-CP}[2-CP_0]} \qquad \text{(Eq. 4.15)}$$

Where [2-CP] is the 2-CP concentration at time t,

k_C is the second-order rate constant in irradiation process,

$K_{2\text{-}CP}$ is the equilibrium adsorption constants of 2-CP onto TiO_2/AC composite, and

$[2\text{-CP}]_0$ is the initial concentration of 2-CP

The photocatalytic degradation of 2-CP in the presence of TiO_2/AC composite exhibits pseudo first-order kinetics with respect to 2-CP concentration as in

$$-\frac{d[2-CP]}{dt} = k_{obs}[2-CP] = k_c \frac{K_{2-CP}}{1+K_{2-CP}[2-CP]_0}[2-CP] \quad \text{(Eq. 4.16)}$$

Where k_{obs} is the observed pseudo first-order rate concentration for the photocatalytic reduction of 2-CP.Therefore, the integration of Eq. 4.16 results in

$$\ln\left(\frac{[2-CP]_0}{[2-CP]}\right) = -k_{obs}t \quad \text{(Eq. 4.17)}$$

Based on Eq. 4.17, the straight-line relationship of $\ln([2\text{-CP}]_0/[2\text{-CP}])$ versus irradiation time, t, was obtained as listed in Table 4.5

Next, the relationship between k_{obs} and $[2\text{-CP}]_0$ from Eq. 4.17 can be expressed with Eq. 4.18

$$\frac{1}{k_{obs}} = \frac{1}{k_C K_{2-CP}} + \frac{[2-CP]_0}{k_c} \quad \text{(Eq. 4.18)}$$

Eq. 4.18 shows that the linear expression also can be obtained by plotting the reciprocal of degradation rate ($1/k_{obs}$) as a function of the initial 2-CP concentration.

To obtain a kinetic value for both k_c and $K_{2\text{-}CP}$, the experiments with initial 2-CP concentration as of 100-300 mg/L were added. The values of k_{obs} from pseudo-first order equation were calculated and shown in Table 4.8.

Figure 4.11 shows that the linear expression also can be obtained by plotting the reciprocal of degradation rate ($1/k_{obs}$) as a function of the initial 2-CP concentration. By means of a least square best fitting procedure, the values of the adsorption equilibrium constant ($K_{2\text{-}CP}$), and the second-order rate constant in irradiation process (k_C) were obtained

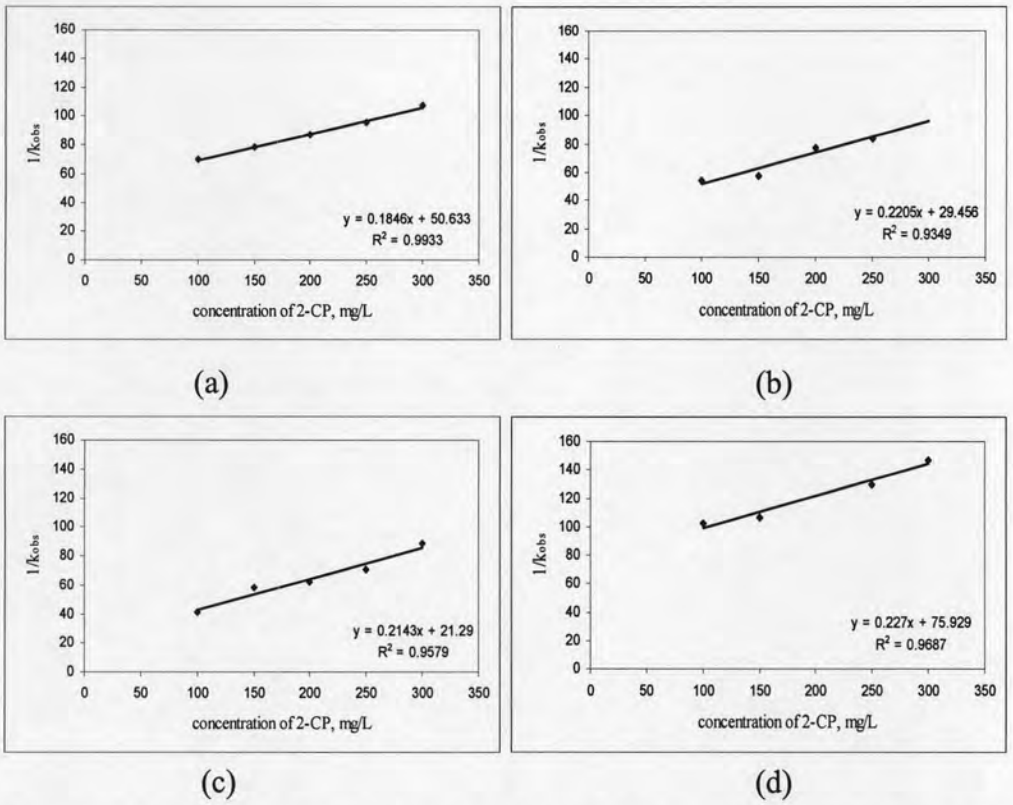

Figure 4.11 Photocatalytic oxidation of 2-CP using TiO_2/O_2, TiO_2/N_2, $TiO_2/AC/N_2$ and TiO_2/P-25 in (a), (b), (c), and (d), respectively

Table 4.9 Values of $K_{2\text{-}CP}$ and k_C from Langmuir-Hinshelwood model for photocatalytic process using TiO_2/O_2, TiO_2/N_2, $TiO_2/AC/N_2$ and TiO_2/P-25

Type of TiO_2 and AC	Equation	$K_{2\text{-}CP}$ (L/mg)	k_c (mg/L-min)	R^2
TiO_2/O_2	y = 0.1846x + 50.633	0.0036	5.4171	0.9933
TiO_2/N_2	y= 0.2205x + 29.456	0.0075	4.5351	0.9349
$TiO_2/AC/N_2$	y = 0.2143x + 21.290	0.0101	4.6664	0.9579
TiO_2/P-25	y = 0.2270x + 75.929	0.0029	4.4053	0.9687

From the results, it was found that the TiO_2/O_2, TiO_2/N_2, $TiO_2/AC/N_2$ and TiO_2/P-25 prepare at 500°C as calcination temperature showed the composites which synthesized by nitrogen adsorption method have more efficiency than that synthesized by oxygen adsorption or the commercial TiO_2. In comparison of all composite

materials by the $K_{2\text{-}CP}$ and k_c values, it was shown that $TiO_2/AC/N_2$ provides the highest $K_{2\text{-}CP}$ value. From this experiment part, $TiO_2/AC/N_2$ is the best material in providing the highest efficiency in photocatalytic process, and the 2-CP removal efficiency of all materials can be ordered as $TiO_2/AC/N_2$ > TiO_2/N_2 > TiO_2/O_2 > TiO_2/P-25. The adsorption step in photocatalysis process plays the major role in the increasing of $TiO_2/AC/N_2$ as seen by the increasing tends of $K_{2\text{-}CP}$

4.2 Effect of different calcination temperature of TiO_2/N_2, $TiO_2/AC/N_2$ composite

4.2.1 Effect of different calcination temperatures on nanocrystal TiO_2/N_2, $TiO_2/AC/N_2$ composite

As the molar ratios of TTiP: AC in nanocrystal TiO_2/AC composite synthesis affects the TiO_2 properties, the gain growth pattern of TiO_2/AC composite would be changed with the variation of calcination temperatures on nanocrystal TiO_2/AC composite. The molar ratios of TTiP: AC were fixed at 1:0, 1:10, and 0:1 and the calcination time was 30 min, the calcination temperature was varied as 500°C, 800°C, 1100°C and 1300°C. A set of TiO_2/AC composite nanoparticles prepared in the molar ratios of 1:0, 0:1 were also calcined at the above temperatures for comparisons. The crystal structures of TiO_2/AC composite from each condition obtain from x-ray diffraction are illustrated in Figure 4.12 and 4.13.

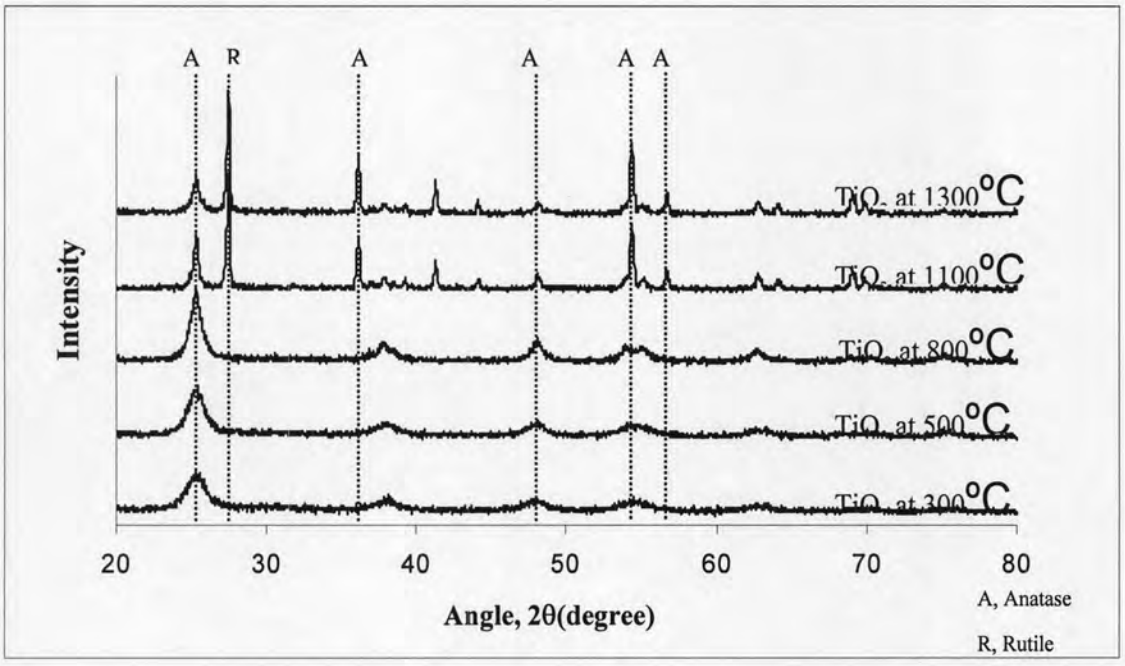

Figure 4.12 XRD patterns showing crystal structures of TiO_2/N_2 in different calcination temperatures

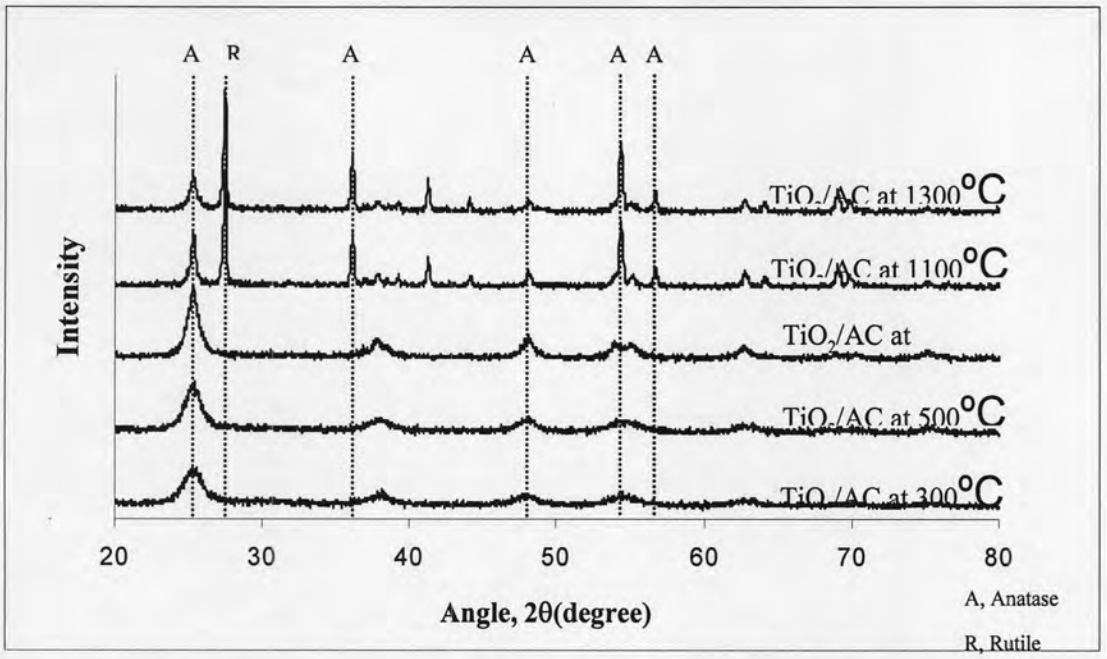

Figure 4.13 XRD patterns showing crystal structures of $TiO_2/AC/N_2$ composite in different calcination temperatures

As shown in Figure 4.12 and 4.13, anatase phase with a major peak corresponding to (1011) was the predominant structure for the TiO_2/AC composite, calcined at 500°C -1300°C. The growth of anatase was increased with the higher calcination temperatures as shown in Figure. Rutile phase with a major peak corresponding to (1101) was developed with the 1100°C-1300°C calcination temperatures while the intensity corresponding to the anatase phase was reduced sharply. It is worth to note that the transformation of anatase to rutile phase of TiO_2/AC composite in the molar ratio of 1:0 and 1:10 were developed at 1000°C.

Percentages of anatase and rutile phases were also calculated to compare the phase transformation of TiO_2/AC composite in each molar ratio as shown in Table 4.10.

Table 4.10 Percentage of anatase and rutile phase in samples obtained from different calcination temperatures

Calcination Temperations (°C)	TiO_2/AC [1:0]		TiO_2/AC [1:10]	
	Anatase (%)	Rutile (%)	Anatase (%)	Rutile (%)
500	100.00	0.00	100.00	0.00
800	100.00	0.00	100.00	0.00
1100	32.07	67.93	84.15	15.85
1300	18.65	81.35	52.95	47.05

The surface morphologies of TiO_2/AC composite nanocrystals from some conditions are shown in Figure 4.14 (a)–(d). There is no obvious surface morphological difference with the different calcination temperatures in the range of 500°C-1300°C. When observe the percentage of anatase to rutile, it was found that $TiO_2/AC/N_2$ have more percentage of anatase and rutile than in TiO_2/N_2. The percentage of anatase was increased with the increasing of calcination temperature.

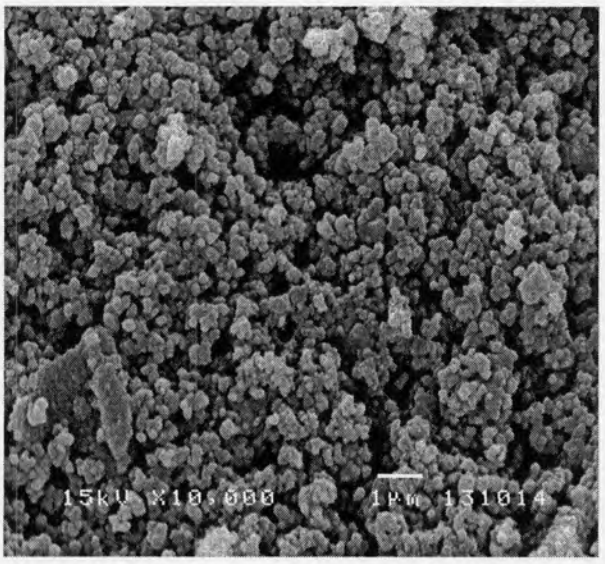

(a) TiO_2/N_2 at 500 °C

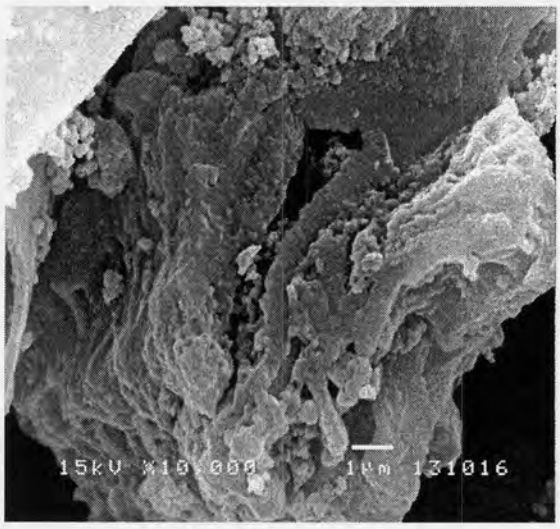

(b) $TiO_2/AC/N_2$ at 500 °C

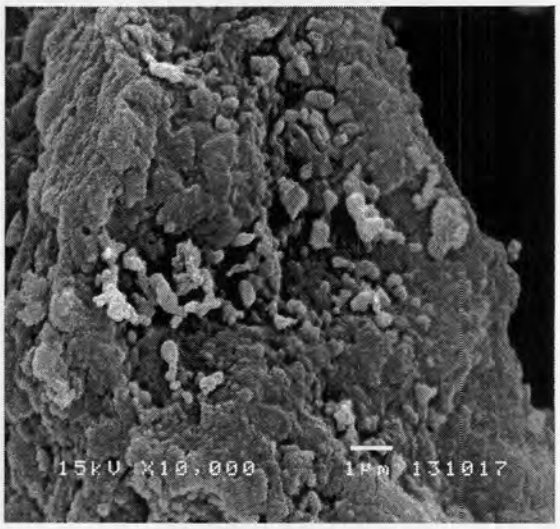

(c) $TiO_2/AC/N_2$ at 1100 °C

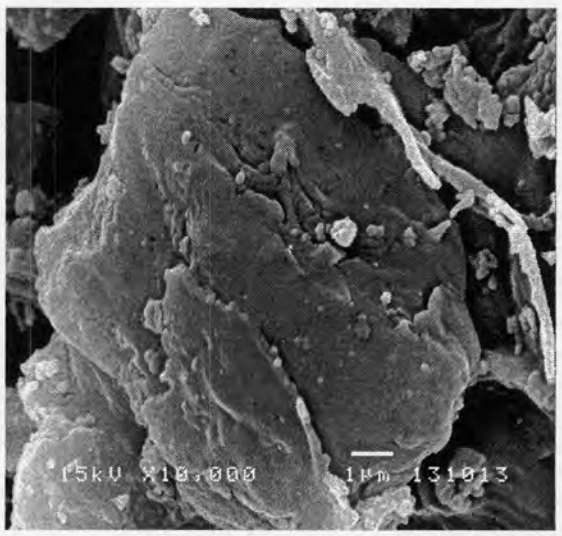

(d) AC/N_2 at 500 °C

Figure 4.14 SEM images showing surface morphology of TiO_2/AC composite nanocrystal

The determinations of all composite materials that have the growth of nanocrystal TiO_2/AC composite are dependent on the calcination temperature. However, when the calcination temperature increased to 1300°C, the sized of nanocrystal TiO_2/AC composite was significant bigger than those obtained from the lower calcination temperatures.The sizes of nanocrystal TiO_2/AC composite from each condition were calculated using Debye-Scherrer equation. Summary of size variation of TiO_2/AC composite nanocrystal synthesized and the calcination

temperatures is shown in Table 4.11. The size variation of TiO_2/AC composite nanocrystal synthesized is also included in the same table for comparison.

Table 4.11 Sizes of anatase and rutile of TiO_2/N_2, $TiO_2/AC/N_2$ composite in sample prepared at different calcination temperatures.

Calcination Temperatures (°C)	TiO_2/N_2		$TiO_2/AC/N_2$	
	Anatase (nm)	Rutile (nm)	Anatase (nm)	Rutile (nm)
500	7.80	-	8.88	-
800	9.79	-	10.14	-
1100	15.62	19.53	10.14	3.91
1300	15.62	19.53	13.02	7.81

As shown in the table, the particle size increases with increasing calcination temperatures. The particles grow slowly at low calcination temperatures and then becomes very fast at high calcination temperatures. The relationship between the particle size and the calcination temperatures in reported here is in agreement with the results reported in various works (Li et al, 2002).

When the calcination temperature is high, the activation energy is very small and the growth rate is large. Thus, the particle size increases very quickly as the calcination temperature increased. In contrast, when the calcination temperature is low, the activation energy is very large and the growth rate becomes slow. Therefore, the grain size increases very slowly as the calcination temperature increase (Li et al., 2002)

It is worth ntoing that the grain size of anatase is normally smaller than rutile. As discussed previously, when the calcination temperature is lower than 1100°c, the phase of TiO_2/AC was fully anatase, while phase of $TiO_2/AC/N_2$ contained both anatase and rutile. This difference in phase of TiO_2/AC is expected to be the cause of the difference in the properties of nanosize TiO_2/AC composite.

4.2.2 Determination of adsorption isotherm of TiO_2/N_2, $TiO_2/AC/N_2$, and AC/N_2 composite in different calcination temperatures.

To obtain the adsorption characteristics of TiO_2/AC composite, it is necessary to determine the adsorption isotherm of the titania. The best condition from the previous section TiO_2/N_2, $TiO_2/AC/N_2$, and AC/N_2 and the range of calcination temperatures are 500°C-1300°C is used in this part. The adsorption of 2-CP with TiO_2/AC composite as the initial concentration of 2-CP varied in the range of 100-300 mg/L was conducted. The results of this experimental part are shown in Figure 4.18-4.20. It is obvious that the amount of 2-CP adsorbed on titania surface is increased with increasing initial concentration of 2-CP in the water.

To obtain the adsorption isotherm of TiO_2/AC composite, the plot of adsorbed 2-CP on titania surface, mg 2-CP/g TiO_2/AC composite versus the concentration of 2-CP in the solution after reaching the equilibrium (mg/L) was performed as shown in Figure 4.15-4.17. The value of adsorbed 2-CP on titania surface was increased with increasing of 2-CP initial concentrations and the plateau of the adsorption pattern was obtained.

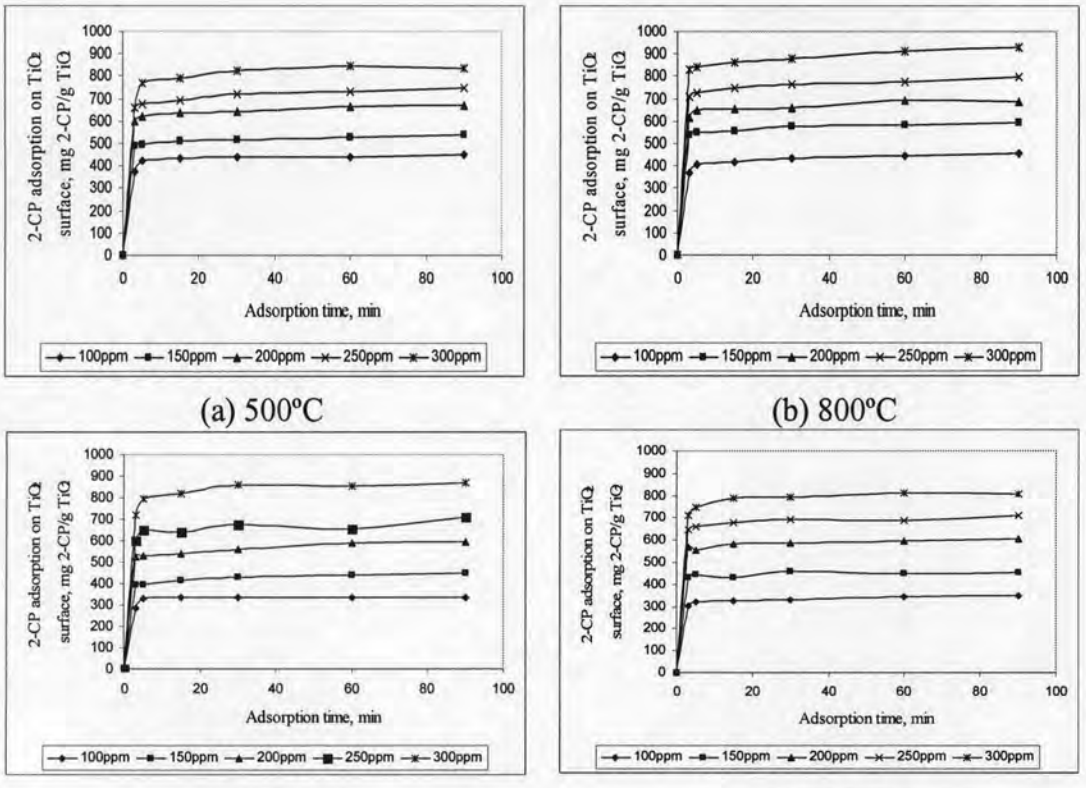

(a) 500°C (b) 800°C

(c) 1100°C (d) 1300°C

Figure 4.15 Adsorption of 2-CP on the TiO_2/N_2 surface (mg 2-CP/ g TiO_2) in (a), (b), (c), and (d), respectively.

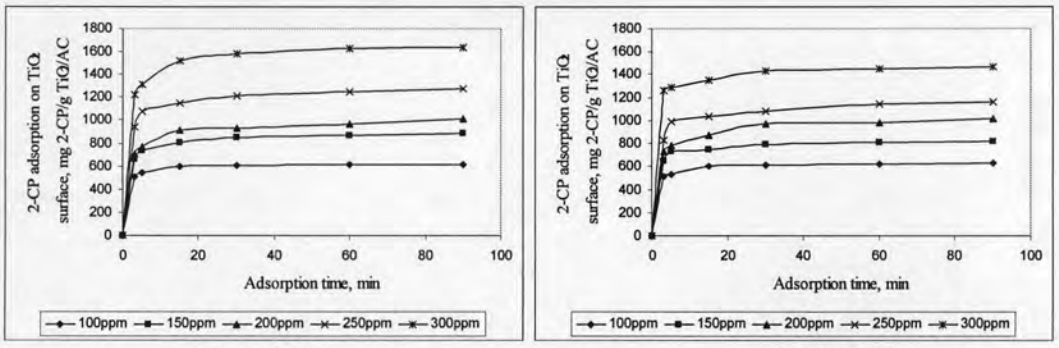

(a) 500°C (b) 800°C

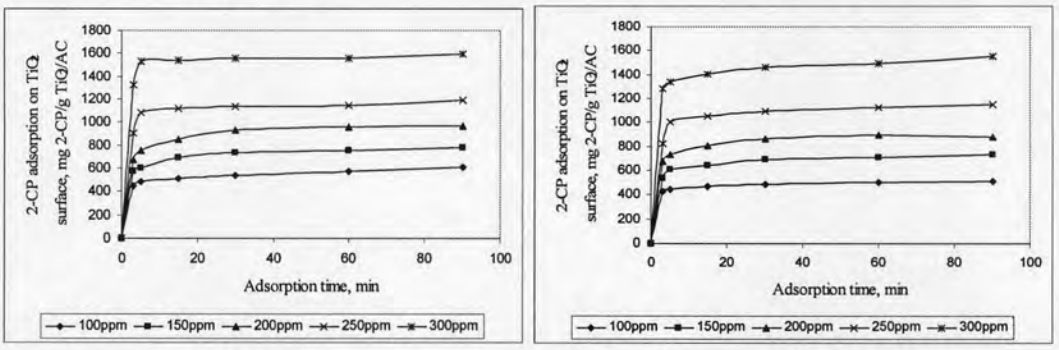

(c) 1100°C (d) 1300°C

Figure 4.16 Adsorption of 2-CP on the $TiO_2/AC/N_2$ surface (mg 2-CP/ g TiO_2/AC) in (a), (b), (c), and (d), respectively.

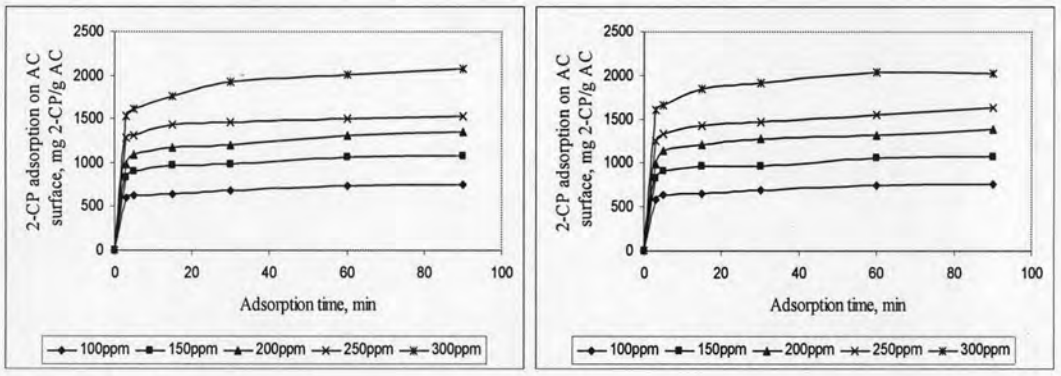

(a) 500°C (b) 800°C

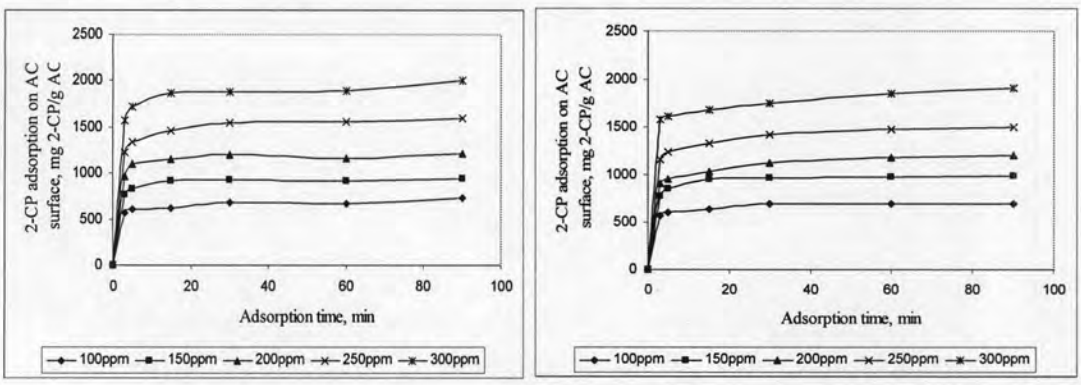

(c) 1100°C (d) 1300°C

Figure 4.17 Adsorption of 2-CP on the AC/N_2 surface (mg 2-CP/ g AC) in (a), (b), (c), and (d), respectively.

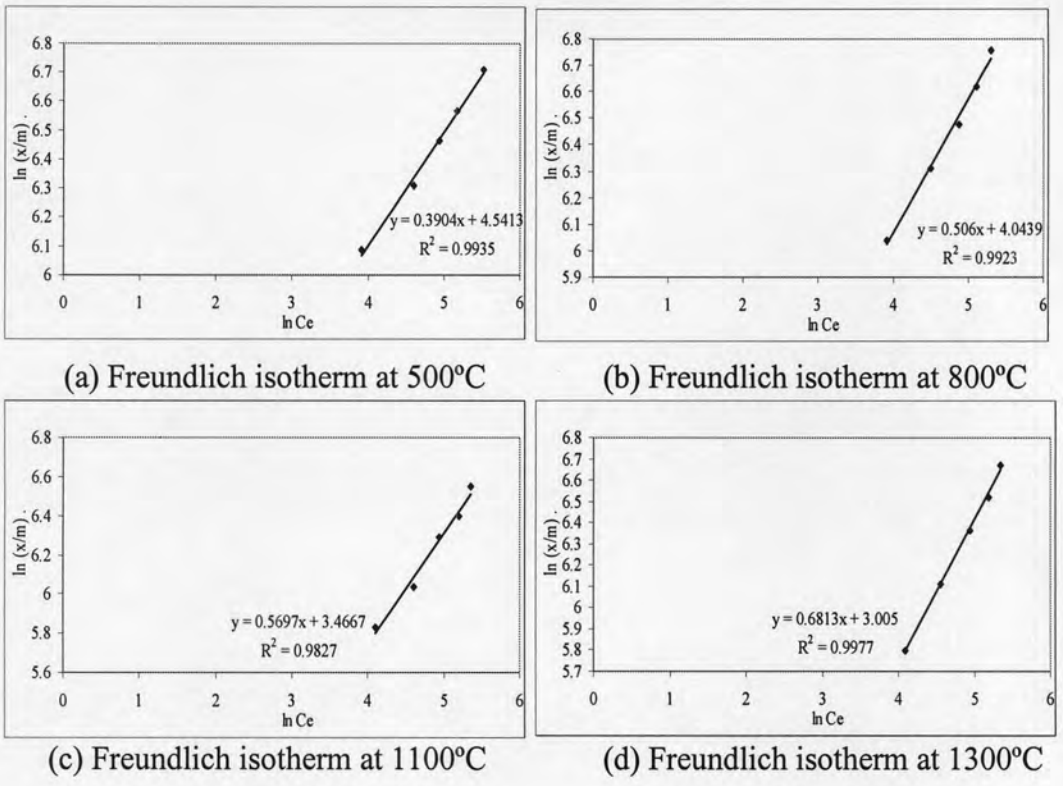

(a) Freundlich isotherm at 500°C (b) Freundlich isotherm at 800°C

(c) Freundlich isotherm at 1100°C (d) Freundlich isotherm at 1300°C

Figure 4.18 Freundlich Isotherm of TiO_2/N_2 in different calcination temperatures in (a), (b), (c), and (d), respectively.

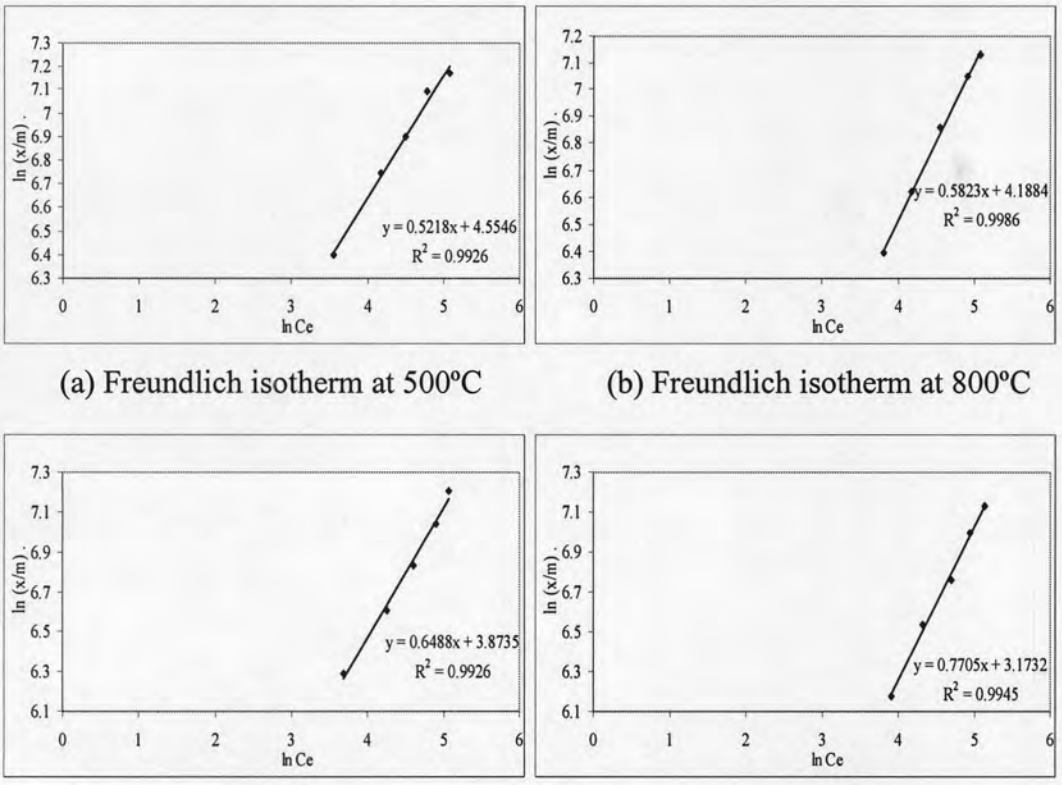

(a) Freundlich isotherm at 500°C (b) Freundlich isotherm at 800°C

(c) Freundlich isotherm at 1100°C (d) Freundlich isotherm at 1300°C

Figure 4.19 Freundlich Isotherm of $TiO_2/AC/N_2$ in different calcination temperatures are shown in (a), (b), (c), and (d), respectively.

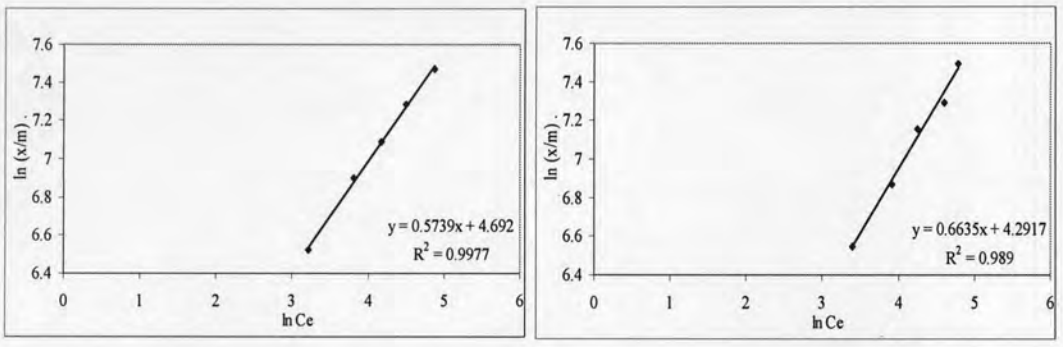

(a) Freundlich isotherm at 500°C (b) Freundlich isotherm at 800°C

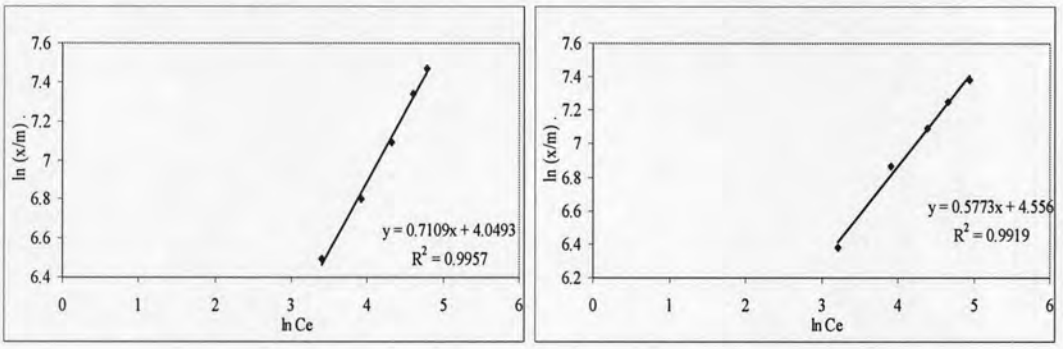

(c) Freundlich isotherm at 1100°C (d) Freundlich isotherm at 1300°C

Figure 4.20 Freundlich Isotherm of AC/N_2 in different calcination temperatures in (a), (b), (c), and (d), respectively.

The expressed equation of TiO_2/N_2 in the molar ratio of 1:0 in 500°C calcination temperature is

$$\ln(x/m) = 0.4257\ln C_e + 4.3786 \qquad \text{(Eq. 4.18)}$$

The correlation coefficient for the Freundlich plot was found to be 0.9617, where the Freundlich constant k_f and n were found to be 1.4767 and 2.3491, respectively. This was more than that from the Langmuir plot. The value of correlation coefficient of 2-CP adsorption indicates that the adsorption behavior of 2-CP onto TiO_2/AC composite tends to be a multilayer adsorption as described by the Freundlich isotherm rather than the Langmuir isotherm.

Equation and constants of TiO_2/N_2, $TiO_2/AC/N_2$ and AC/N_2 in different calcination temperatures were used the same calculation method ad shown above and the values are shown in table 4.12.

Table 4.12 Freundlich equation of TiO_2/N_2 in different calcination temperature

Calcination temperature (°C)	Equation	R^2	k_f	n
500	Y=0.4257x+4.3786	0.9617	1.4767	2.3491
800	Y=0.5060x+4.0439	0.9923	1.3972	1.9763
1100	Y=0.5697x+3.4667	0.9827	1.2432	1.7553
1300	Y=0.6813x+3.0050	0.9977	1.1003	1.4678

The calcinations of $TiO_2/AC/N_2$ in different calcination temperature used the same method in the Freundlich equation that are following;

Table 4.13 Freundlich equation of $TiO_2/AC/N_2$ in different calcination temperature

Calcination temperature (°C)	Equation	R^2	k_f	n
500	Y=0.5218x+4.5516	0.9926	1.4932	1.8318
800	Y=0.5823x+4.1884	0.9986	1.4323	1.7173
1100	Y=0.6488x+3.8735	0.9926	1.3542	1.5413
1300	Y=0.7705x+3.1732	0.9945	1.1547	1.2978

The calcinations of AC/N_2 in different calcination temperature used the same method in the Freundlich equation that are following;

Table 4.14 Freundlich equation of AC/N_2 in different calcination temperature

Calcination temperature (°C)	Equation	R^2	k_f	n
500	Y=0.5547x+4.8025	0.9769	1.4612	1.5337
800	Y=0.6635x+4.2917	0.9890	1.4567	1.5072
1100	Y=0.7109x+4.0493	0.9957	1.3985	1.4067
1300	Y=0.5773x+4.5560	0.9919	1.5164	1.7322

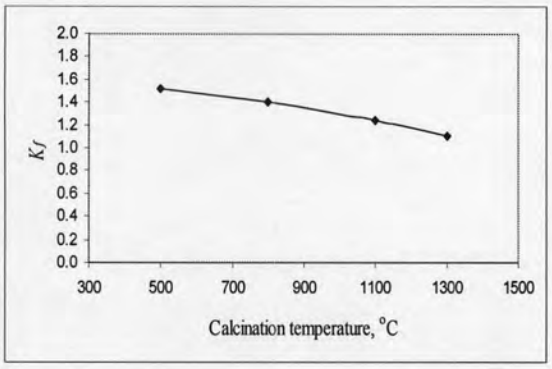

(a) K_f constant of TiO_2/N_2

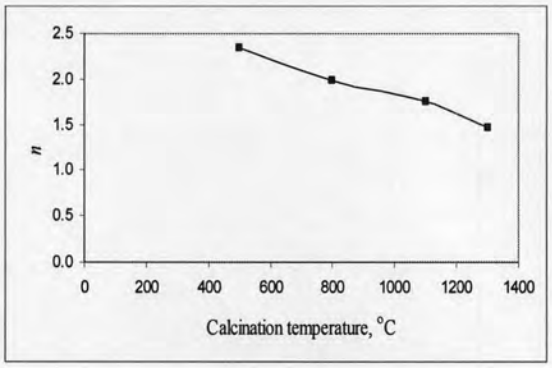

(b) n constant of TiO_2/N_2

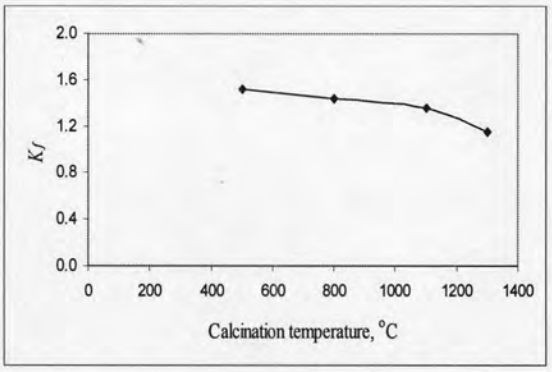

(c) K_f constant of $TiO_2/AC/N_2$

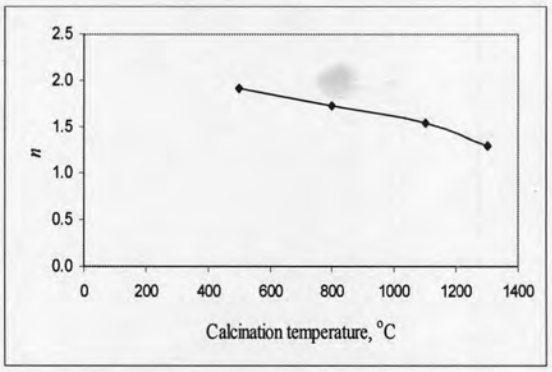

(d) n constant of $TiO_2/AC/N_2$

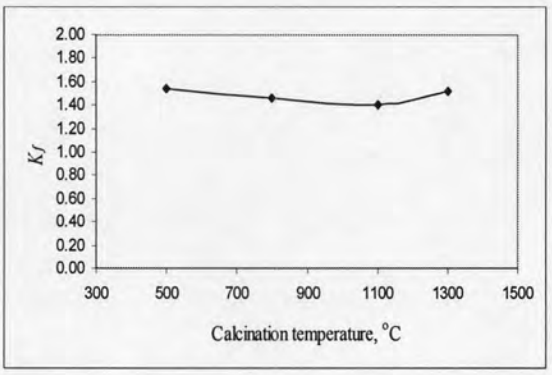

(e) K_f constant of AC/N_2

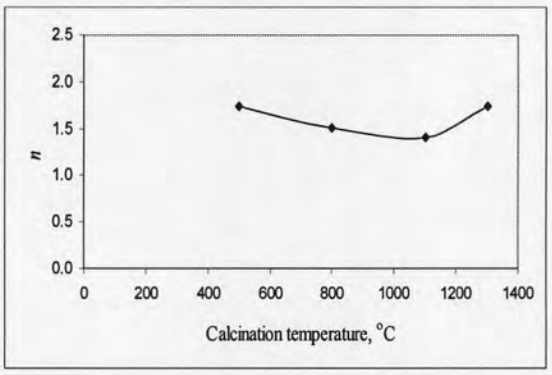

(f) n constant of AC/N_2

Figure 4.21 K_f and n constant of Freundlich isotherm of TiO_2/N_2, $TiO_2/AC/N_2$ and AC/N_2

From this part, it was found that the different calcination temperatures have affects on the molar ratios of TiO_2/N_2, $TiO_2/AC/N_2$ in adsorption behavior. The calcination temperature at 500°C is the best condition in providing highest K_f and n values in adsorption process. From the results found that, when the calcination

temperatures increased, the phase structures were changed, the size and surface area also changed.

The constant of Freundlich adsorption isotherm, the K_f and n were the same tend in TiO_2/N_2 and $TiO_2/AC/N_2$, because the calcination temperature have effects in the same manner. However, in the AC composite, the K_f and n have different pattern with TiO_2/N_2 and $TiO_2/AC/N_2$. It was found that the calcination temperature has no effect on AC. In overall, the K_f and n values tend to decrease with the increasing of the calcination temperature.

4.2.3 Irradiation process of nanocrystal TiO_2/N_2, $TiO_2/AC/N_2$ composite at different calcination temperatures.

Effects of calcination temperature on irradiation process of nanocrystal TiO_2/N_2, $TiO_2/AC/N_2$ composite were studied. In this experimental set, TiO_2/N_2, $TiO_2/AC/N_2$ composite nanopowders obtained previously at calcination temperatures in the range of 500°C-1300°C was used and the amount of TiO_2/N_2, $TiO_2/AC/N_2$ composite in each study was fixed at 0.1 g/L.

The highest concentrations of adsorbed 2–CP on TiO_2/AC composite surface using different types of TiO_2/AC composite in adsorption process were determined and shown in Figure 4.22 and 4.24. The photocatalytic reduction of 2–CP under irradiation process for the nanocrystal TiO_2/N_2 and $TiO_2/AC/N_2$ composite with different molar ratios of TTiP/AC was also compared and the ratio of residual to initial concentration of 2–CP in term of C/C_0 as a function of irradiation time was illustrated in Figure 4.23 and 4.25. It was found that the contact time to reach the equilibrium was 90 minutes. The equilibrium concentrations of 2–CP in the aqueous solution using different types of TiO_2/AC composite were considerably different. The 2–CP adsorption of TiO_2/N_2, $TiO_2/AC/N_2$ and AC/N_2 in different calcination temperatures were in the range of 790-900, 1,250-1,450, and 1,600-1,910 mg 2–CP/g TiO_2/AC, respectively.

It is obvious that the nanocrystal TiO_2/AC composite prepared at 500°C calcination temperature provided the highest efficiency in 2-CP removal compared to the other conditions. It is worth to note that the TiO_2/AC composite in the molar ratio of 1:10 with 500°C calcination temperature provided the highest amount of 2–CP adsorption on titania surface, while the TiO_2/AC composite with 500°C calcination temperature provided the highest amount of 2–CP reduction upon irradiation process

This may be due to the fact that crystal phase of TiO_2/AC in the molar ratios of 1:0 and 1:10 at the 500°C calcination temperature was pure anatase phase with highest amount of TiO_2 in the crystal compare to those obtained from the other calcination temperature as shown by XRD pattern in Figure 4.12-4.13.

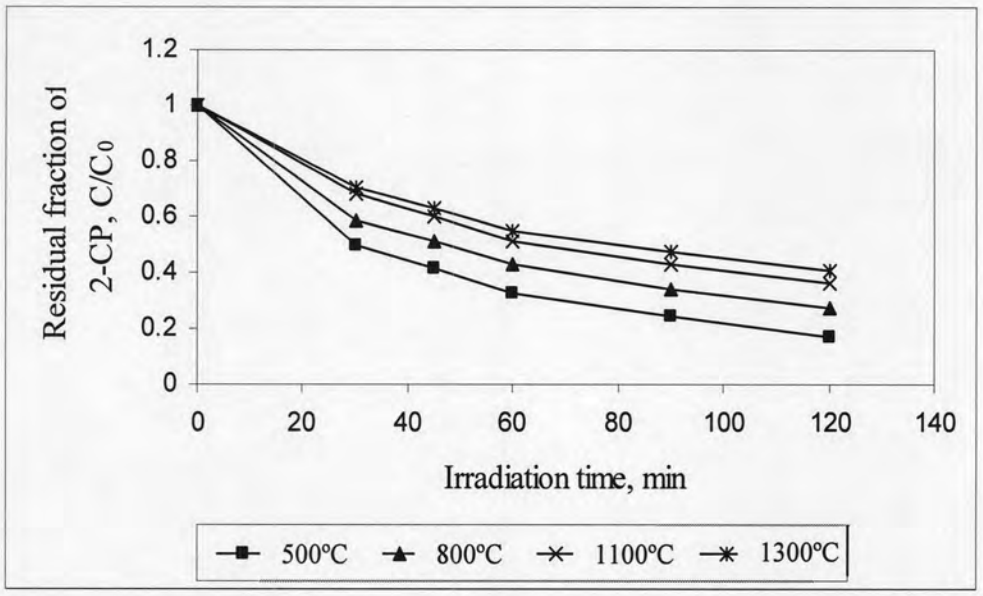

Figure 4.22 Photocatalytic oxidation of 2-CP by using TiO_2/N_2 composite prepare at different calcination temperature

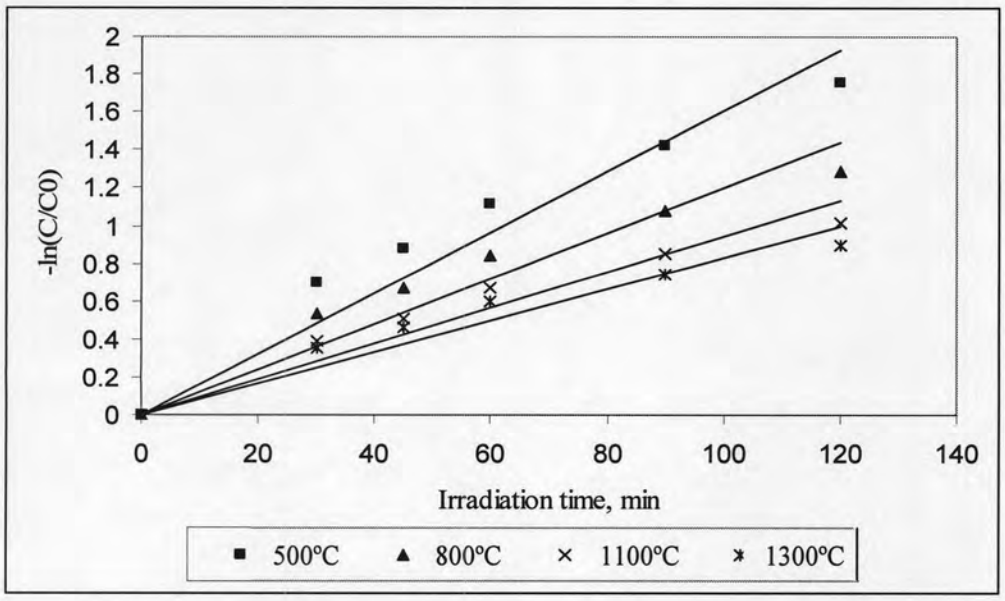

Figure 4.23 Value of k_{obs} from the photocatalytic process of removal 2-CP by using TiO_2/N_2 composite in different calcination temperature

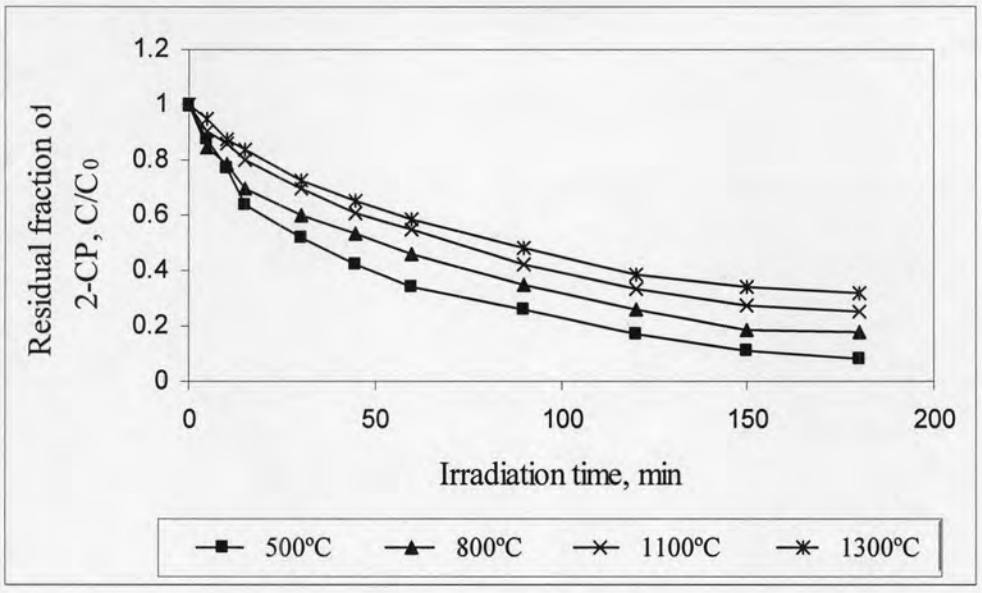

Figure 4.24 Photocatalytic oxidation of 2-CP by using $TiO_2/AC/N_2$ composite prepare at different calcination temperature

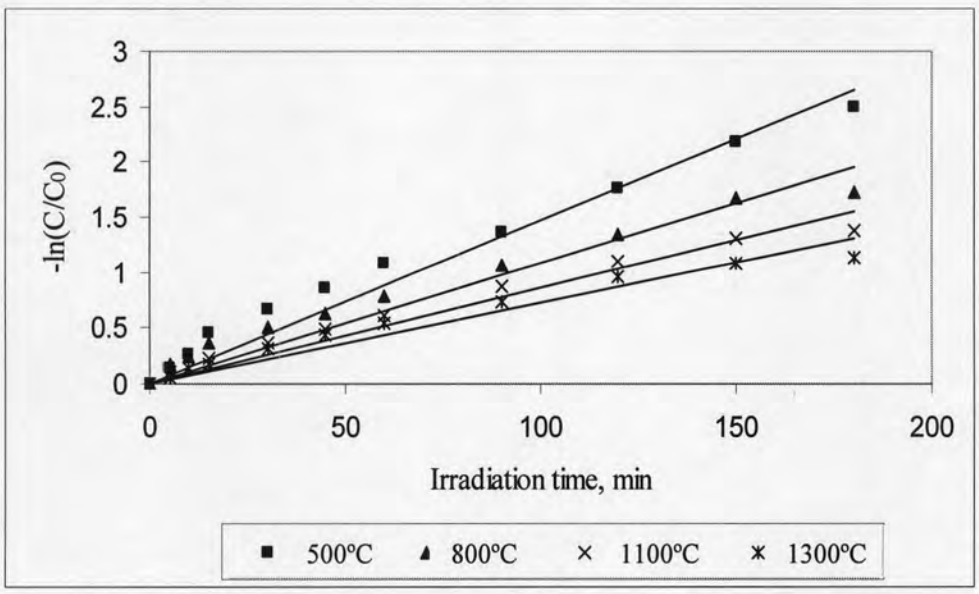

Figure 4.25 Value of k_{obs} from the photocatalytic process of removal 2-CP by using $TiO_2/AC/N_2$ composite in different calcination temperature

In terms of kinetic study, the photocatalytic oxidation reaction of 2–CP of nanocrystal TiO_2/AC composite obtained from various calcination temperatures were followed the first-order pattern. The values of k_{obs} were calculated and the plots of k_{obs} as a function of calcination temperature, as shown in Figure 4.26. This figure shows that k_{obs} of TiO_2/AC in the molar ratios of 1:0 and 1:10 increased with increasing calcination from 500°C-800°C and starting decreased with increasing calcination temperature from 800°C-1300°C. From this information, the

photocatalytic activity are represented by the k_{obs} was mainly governed by the anatase phase of TiO_2/AC composite. As the amount of anatase TiO_2/AC composite increased with calcination temperature, the photocatalytic activity increased. At calcination temperature higher than 1100°C, crystal phase was transformed to rutile, causing the decreased of photocatalytic activity. It is worth to note that in the photocatalysis process, the photocatalytic oxidation reduction process during irradiation is much more the major mechanism in contaminant removal than the adsorption process at the beginning step. Thus, in overall consideration, The TiO_2/AC composite in the molar ratio of TiO_2/N_2, TiO_2/AC/N_2 with 500°C calcination temperature provided the best condition for 2–CP removal.

Table 4.14 Value of k_{obs} and 2–CP removal efficiencies of TiO_2/N_2 prepared from different calcination temperature

Calcination temperatures (°C)	k_{obs}	R^2	% Removal
500°C	0.0160	0.9346	92.72
800°C	0.0120	0.9132	84.10
1100°C	0.0094	0.9339	75.99
1300°C	0.0083	0.9199	68.81

Table 4.15 Value of k_{obs} and 2–CP removal efficiencies of TiO_2/AC/N_2 prepared from different calcination temperature

Calcination temperatures (°C)	k_{obs}	R^2	% Removal
500°C	0.0158	0.9484	91.79
800°C	0.0120	0.9619	81.11
1100°C	0.0096	0.9809	74.60
1300°C	0.0083	0.9797	68.04

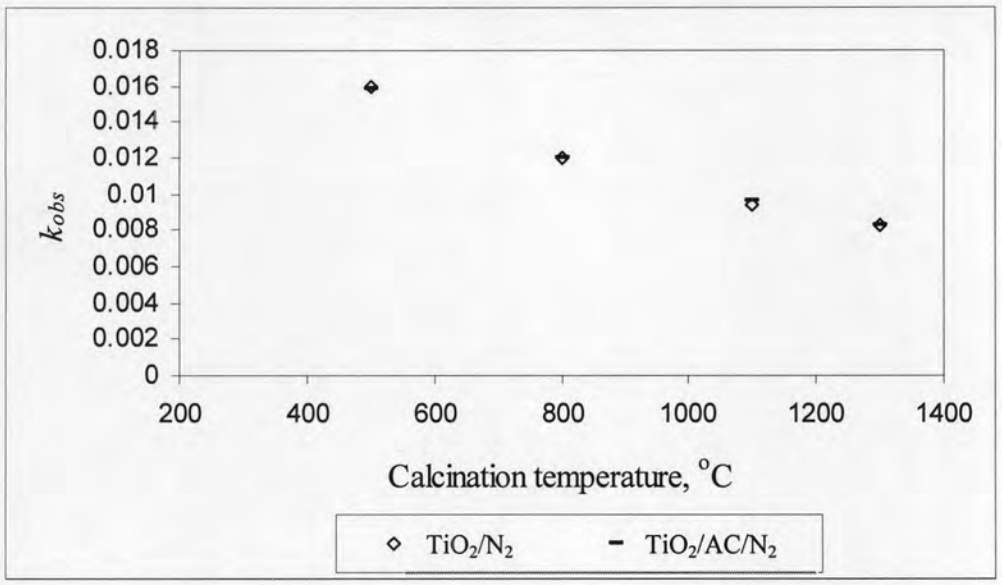

Figure 4.26 k_{obs} of TiO_2/N_2 and $TiO_2/AC/N_2$ in different calcination temperature

4.2.4 Photocatalytic activity of nanocrystal TiO_2/N_2 and $TiO_2/AC/N_2$ composite with different calcination temperature

As mentioned earlier the whole photocatalytic process is concluding with the adsorption part and Irradiation part. The graph below shows both processes in 2-CP removal by using TiO_2/N_2 and $TiO_2/AC/N_2$ composite materials.

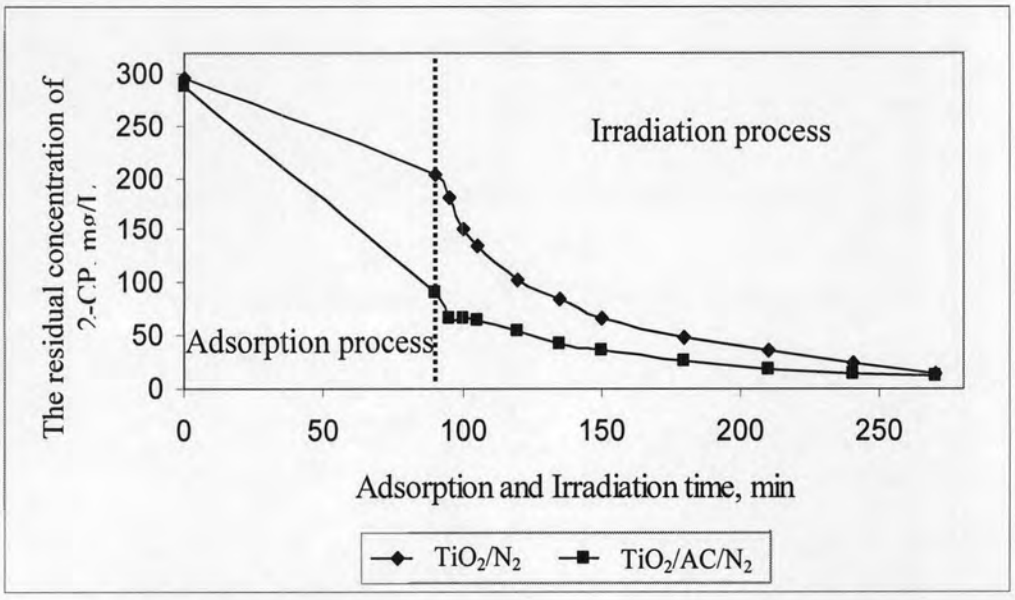

Figure 4.27 Whole processes in photocatalytic process in 2-CP removal by using TiO_2/N_2 and $TiO_2/AC/N_2$ composite, in both adsorption and irradiation time.

During the first period in the adsorption part, $TiO_2/AC/N_2$ removes 2-CP faster than TiO_2/N_2. However at in the end of irradiation part both composite have a similar residual concentration. From this result, $TiO_2/AC/N_2$ has more efficiency in adsorption part and TiO_2/N_2 has more efficiency in irradiation part. However, when both the photocatalytic process using these two materials reached the end of process, there is a similar residual concentration of 2-CP in the solution.

It is worth to note that the pure TiO_2 in TiO_2/N_2 used in this experiment was 0.1 g, while the TiO_2 in $TiO_2/AC/N_2$ was 0.0285 g in the total weight of 1.0 g of $TiO_2/AC/N_2$. The experimental data here showed that with addition of small amount of TiO_2 to the AC the increasing of 2-CP efficiency is pronounced.

4.3 Mineralization of 2-CP by using TiO_2/N_2 and $TiO_2/AC/N_2$ composite

4.3.1 Determination of mineralization of 2-CP by the total organic carbon from the residual concentration of 2-CP by using the TOC method

The total organic carbon from the residual concentration of 2-CP by using TiO_2/N_2 and $TiO_2/AC/N_2$ is shown in Figure 4.28. The initial concentrations of 2-CP was about 300 mg/L. The photocatalytic process included 90 minute adsorption process and 180 minute irradiation process. The samples were taken out 0 and 90 min for adsorption time and 0, 30, 60, 90, 120 , 150 and 180 minute for irradiation time as shown in figure below;

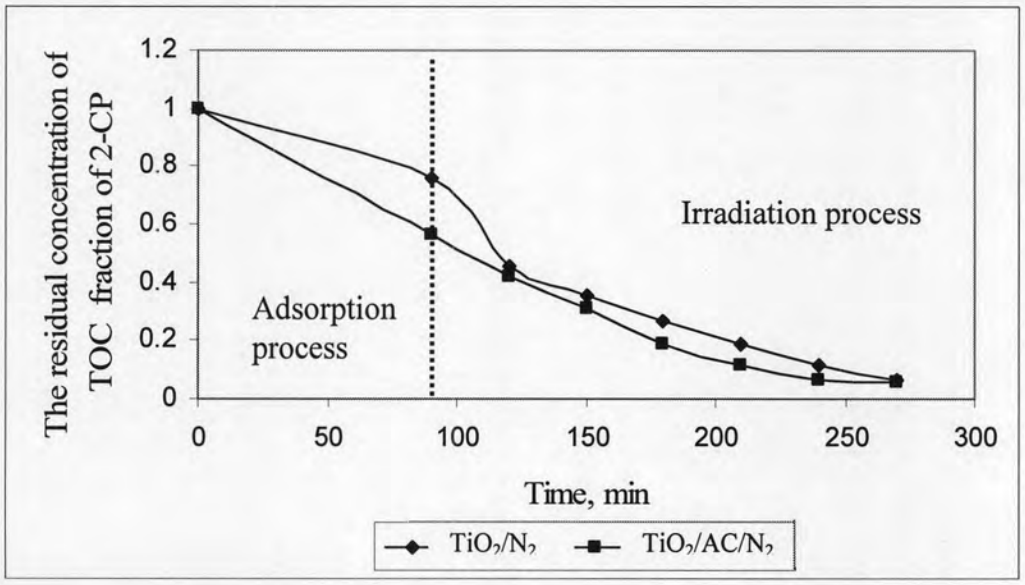

Figure 4.28 C/C_0 of the residual concentration of TOC fraction of 2-CP by using TiO_2/N_2 and $TiO_2/AC/N_2$ composite in both adsorption and irradiation time.

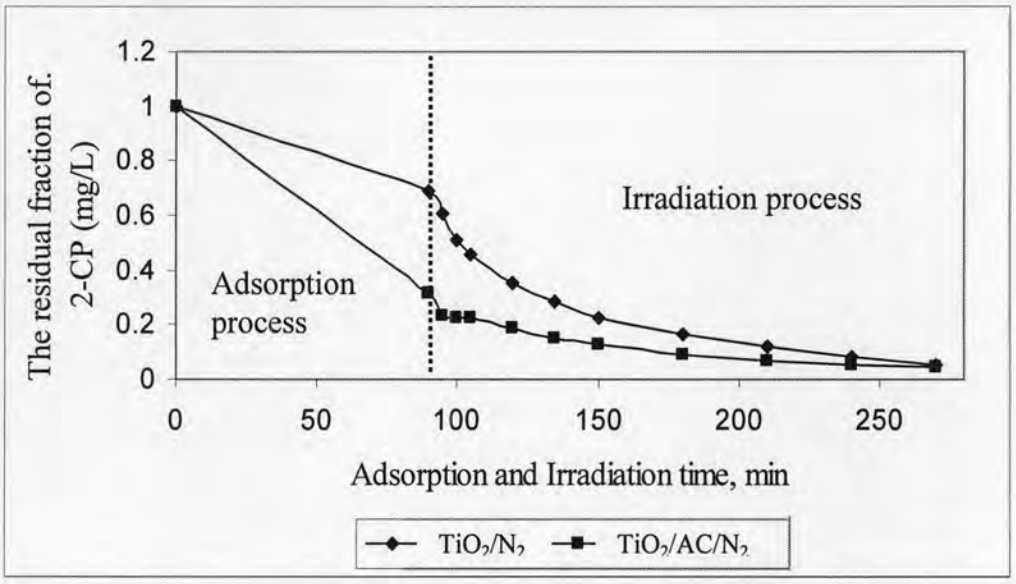

Figure 4.29 C/C_0 of the residual fraction of 2-CP removal by using TiO_2/N_2 and $TiO_2/AC/N_2$ composite, in both adsorption and irradiation time.

From figures, the C/C_0 of residual concentrations of TOC fraction of 2-CP by using TiO_2/N_2 and $TiO_2/AC/N_2$ composite were compared with the residual concentration fraction (C/C_0) of 2-CP from the colorimetric method. It shows that the C/C_0 of residual concentration of TOC fraction similar with the residual concentration fraction (C/C_0) of 2-CP from the colorimetric method. This result suggested that the residual concentrations (C/C_0) by TOC method might come from the total residual concentration of 2-CP. To obtain more information, the determination of 2-CP intermediate during photocatalytic process using Gas Chromatography/Mass Spectrometry (GC/MS) was performed as shown in the next section.

4.3.2 Determination of the intermediate from Gas Chromatography/Mass Spectrometry (GC/MS)

In this part, the intermediate occured during photocatalysis process was determined by using GC/MS. For this intermediate analysis, the samples were taken at the starting period of photocatalysis process until it reached the end of the process. The initial concentration of 2-CP was about 300 mg/L and the irradiation was 3 hours. In this part, the TiO_2/AC materials synthesized with the molar ratios of TiO_2/AC as 1:0 and 1:10 under 500°C for calcination temperature were selected for intermediate analysis. The results of GC/MS after 180 min irradiation time using TiO_2/N_2 and TiO_2/AC are shown in Figure 4.30 and 4.31, respectively.

Conditions for GC-MS in the single-column analysis of the underivatized phenol

Column	DB-5
Carrier gas:	Nitrogen
Flow rate:	6 mL/min
Makeup gas:	Hydrogen
Flow rate:	30 mL/min
Temperature program:	1.5 min hold
	80°C to 230°C at 6°C/min
	230°C to 275°C at 10°C/min
	45 min hold
Injector temperature:	200°C
Detector temperature:	300°C
Detector type:	MSD

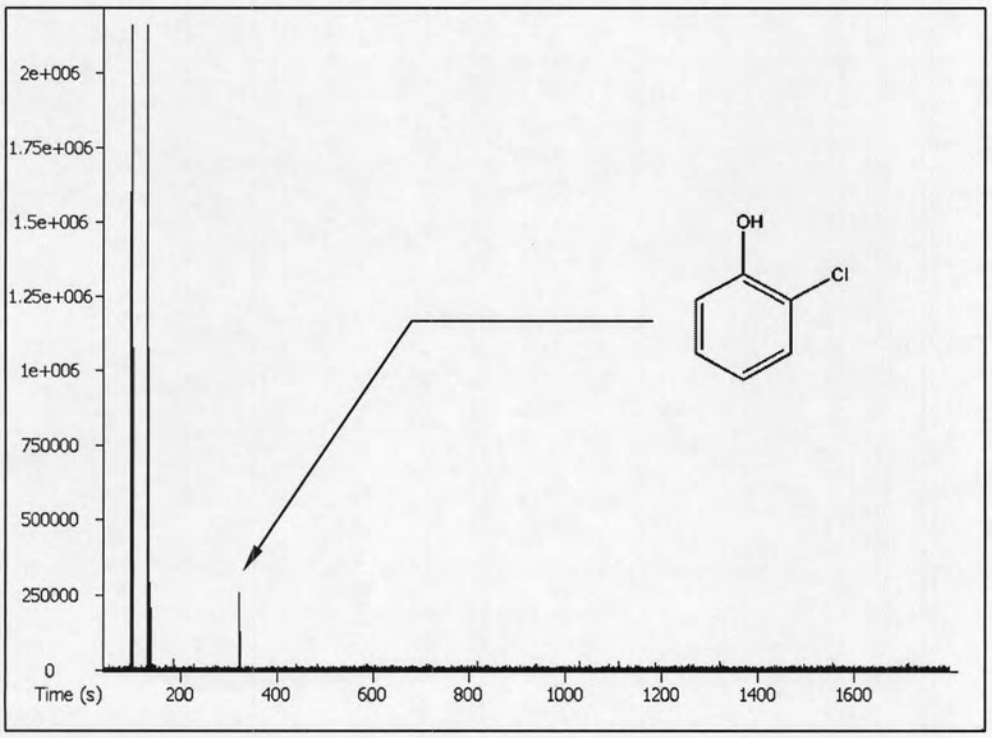

Figure 4.30 Showing the result of 2-CP after180 min irradiation time by using TiO_2/N_2 of irradiation process from GC/MS

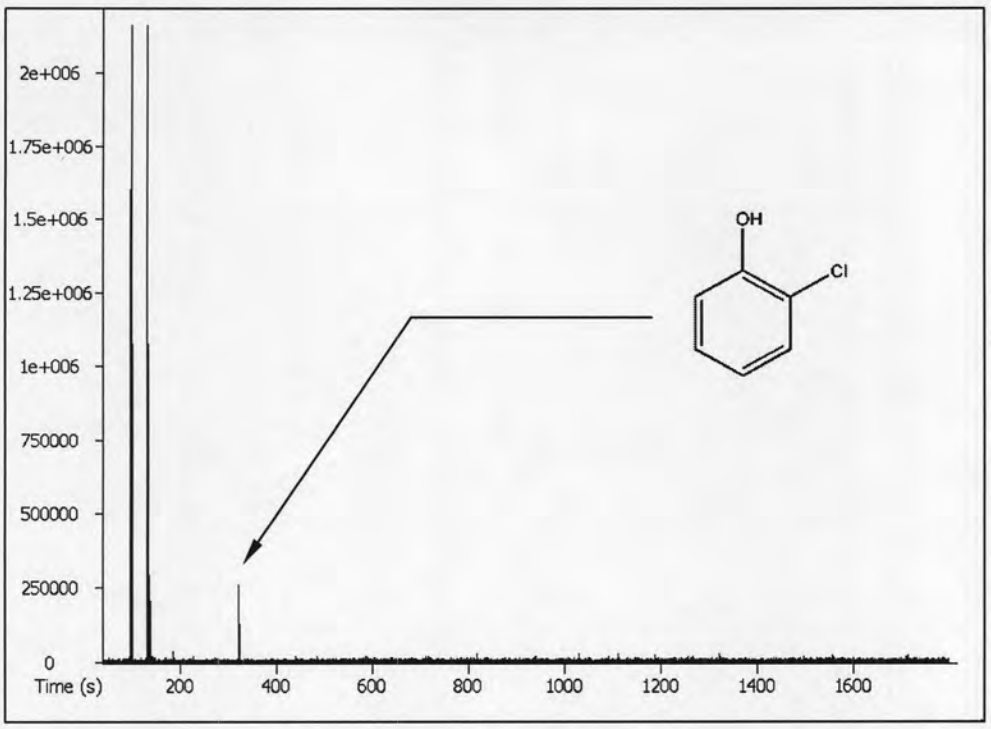

Figure 4.31 Result of 2-CP after180 min irradiation time by using $TiO_2/AC/N_2$ from GC/MS

It was found that no intermediate was detected in the residual concentration by using GC/MS. This result is in agreement with the result from TOC analysis. That the residual concentration(C/C_0) of 2-CP from UV-VIS spectrophotometer and the result from the TOC analysis that from only the residual concentration of 2-CP in the water not from any intermediate. Owing to photocatalysis process by using TiO_2/N_2 and $TiO_2/AC/N_2$ composite as the catalyst, the occurring of intermediate that quickly degrades as fast as and can not be detected. It was supported by the previous research (Sivalingam et al., 2004), which investigated kinetic of the degradation in each type of phenol by using synthesis TiO_2 by calcination process as the catalyst. It was found that the fast occurring of the degradation resulting in non-detected intermediate during photocatalysis process.